Novel epoxy-tiglianes stimulate skin keratinocyte wound healing responses and re-epithelialization via protein kinase C activation

Rachael L. Moses[a], Glen M. Boyle[b], Rachel A. Howard-Jones[c], Rachel J. Errington[c], Jenny P. Johns[b], Victoria Gordon[d], Paul Reddell[d], Robert Steadman[e], Ryan Moseley[a*].

[a]Regenerative Biology Group, School of Dentistry, Cardiff Institute of Tissue Engineering and Repair (CITER), College of Biomedical and Life Sciences, Cardiff University, UK. [b]Cancer Drug Mechanisms Group, QIMR Berghofer Medical Research Institute, Brisbane, Queensland, Australia. [c]Tenovus Institute, School of Medicine, College of Biomedical and Life Sciences, Cardiff University, UK. [d]QBiotics Group, Yungaburra, Queensland, Australia. [e]Welsh Kidney Research Unit, Division of Infection and Immunity, Cardiff Institute of Tissue Engineering and Repair (CITER), School of Medicine, College of Biomedical and Life Sciences, Cardiff University, UK.

***Corresponding Author:** Regenerative Biology Group, School of Dentistry, Cardiff Institute of Tissue Engineering and Repair (CITER), College of Biomedical and Life Sciences, Cardiff University, Cardiff, UK. CF14 4XY.

Tel: +44 (0)29 2251 0649.

Fax: +44 (0)29 2074 6489.

Email: Moseleyr@cardiff.ac.uk

ABSTRACT

Epoxy-tiglianes are a novel class of diterpene esters. The prototype epoxy-tigliane, EBC-46 (tigilanol tiglate), possesses potent anti-cancer properties and is currently in clinical development as a local treatment for human and veterinary cutaneous tumors. EBC-46 rapidly destroys treated tumors and consistently promotes wound re-epithelialization at sites of tumor destruction. However, the mechanisms underlying these keratinocyte wound healing responses are not completely understood. Here, we investigated the effects of EBC-46 and an analogue (EBC-211) at 1.51 nM-151 μM concentrations, on wound healing responses in immortalized human skin keratinocytes (HaCaTs). Both EBC-46 and EBC-211 (1.51 nM-15.1 μM) accelerated G0/G1-S and S-G2/M cell cycle transitions and HaCaT proliferation. EBC-46 (1.51-151 nM) and EBC-211 (1.51 nM-15.1 μM) further induced significant HaCaT migration and scratch wound repopulation. Stimulated migration/wound repopulation responses were even induced by EBC-46 (1.51 nM) and EBC-211 (1.51-151 nM) with proliferation inhibitor, mitomycin C (1 μM), suggesting that epoxy-tiglianes can promote migration and wound repopulation independently of proliferation. Expression profiling analyses showed that epoxy-tiglianes modulated keratin, DNA synthesis/replication, cell cycle/proliferation, motility/migration, differentiation, matrix metalloproteinase (MMP) and cytokine/chemokine gene expression, to facilitate enhanced responses. Although epoxy-tiglianes down-regulated established cytokine and chemokine agonists of keratinocyte proliferation and migration, enhanced HaCaT responses were demonstrated to be mediated via protein kinase C (PKC) phosphorylation and significantly abrogated by pan-PKC inhibitor, bisindolylmaleimide-1 (BIM-1, 1 μM). By identifying how epoxy-tiglianes stimulate keratinocyte healing responses and re-epithelialization in treated skin, our findings support the further development of this class of small molecules as potential therapeutics for other clinical situations associated with impaired re-epithelialization, such as non-healing skin wounds.

Keywords: Keratinocytes, epoxy-tiglianes, re-epithelialization, proliferation, migration, protein kinase C.

Abbreviations

BIM-1, bisindolylmaleimide-1; CCL, chemokine (C-C motif) ligand; CXCL, chemokine (C-X-C motif) ligand; DMSO, dimethyl sulfoxide; DNA, Deoxyribonucleic acid; ECM, extracellular matrix; ELISA, enzyme-linked immunosorbent assay; FDA, US Food and Drug Administration; GEO, Gene Expression Omnibus; HaCaT, human immortalized keratinocytes; IL, interleukin; IPA®, Ingenuity Pathway Analysis; KRT, keratin; MC, mitomycin C; MMP, matrix metalloproteinase; MTT, [3-(4,5-dimethyl-2-thiazolyl)-2,5-diphenyltetrazolium bromide]; PBS, phosphate buffered saline; PKC, protein kinase C; PVDF, polyvinylidene difluoride; RFU, relative fluorescence units; SDS-PAGE, sodium dodecyl sulfate-polyacrylamide gel electrophoresis; SEM, standard error of the mean; TBS, Tris-buffered saline; TNF-α, tumor necrosis factor-α.

1. Introduction

Epoxy-tiglianes are a novel class of diterpene esters isolated from a native Australian rainforest plant, *Fontainea picrosperma* (*Euphorbiaceae*). The prototype epoxy-tigliane, EBC-46 (12-tigloyl-13-(2-methylbutanoyl)-6,7-epoxy-4,5,9,12,13,20-hexahydroxy-1-tigliaen-3-one, now known as tigilanol tiglate), possesses potent anti-cancer properties in pre-clinical syngeneic and xenograft mouse models [1,2]; and is currently under clinical evaluation as a treatment for cutaneous and subcutaneous tumors in humans and domesticated animals [2,3], having recently completed a Phase I/II human dose escalation safety trial [4]. Following intra-tumoral administration, EBC-46 elicits a rapid, but localized, inflammatory response and loss of integrity of the tumor vasculature, leading to hemorrhagic necrosis and subsequent tumor ablation in melanoma, squamous cell carcinoma and other tumor mouse models; mediated at least in part via protein kinase C (PKC) activation [1]. Remarkably, EBC-46 also stimulates exceptional dermal wound healing *in vivo* following tumor destruction, particularly manifested as accelerated wound re-epithelialization and closure over a 1-month period post-treatment [2-3]. However, little is currently known how epoxy-tiglianes induce such favorable epithelial wound healing outcomes.

Wound re-epithelialization is an essential process during normal healing, facilitating wound closure and the restoration of skin barrier function through the re-establishment of the denuded epithelium by epidermal keratinocytes [5,6]. However, intrinsic differences in the functionality of wound keratinocytes, such as the hyper-proliferative nature of supra-basal keratinocytes, their hyper-adhesive/non-migratory phenotypes and dysregulated differentiation/regulatory pathways [7-11]; lead to impaired re-epithelialization and a failure to reinstate barrier integrity. Such events culminate in clinical problems, such as non-healing chronic skin wounds [12,13]. Despite many modalities being available for the treatment or management of chronic wounds, these often offer limited benefit to healing outcomes and

consequently, non-healing or wound recurrence remain common [14,15]. Current pharmaceutical-based therapies are also severely limited, as Regranex® (Becaplermin) is the only FDA (US Food and Drug Administration)-approved pharmaceutical for chronic skin wounds. However, in addition to being restricted for the treatment of diabetic wounds only, significant efficacy and safety issues surround its use [16]. Consequently, there is a significant unmet clinical need for novel and more efficacious pharmaceuticals capable of restoring re-epithelialization and healing in chronic skin wounds [17].

Therefore, in this study, we investigated how epoxy-tiglianes, EBC-46 and an EBC-46 analogue, EBC-211 (produced by a Payne re-arrangement of the epoxide group on the β ring of EBC-46, circled in red, Fig. 1A), modulate such wound healing responses in HaCaT human immortalized keratinocytes, in line with the enhanced wound re-epithelialization clinically observed *in vivo*. Our results demonstrate that both epoxy-tiglianes exert significant stimulatory effects on keratinocyte wound healing responses, facilitated via PKC activation and the downstream manipulation of gene expression profiles in favor of enhanced proliferation and migration. Such findings demonstrate the mechanisms by which epoxy-tiglianes mediate wound re-epithelialization, closure and restoration of skin barrier function following tumor destruction. In addition, the findings advocate the further investigation of this class of small molecules as novel pharmaceutical therapies for other clinical situations associated with impaired re-epithelialization, such as non-healing skin wounds.

2. Materials and methods

2.1. Chemicals, reagents and antibodies

EBC-46 and EBC-211 were provided by QBiotics Group (Yungaburra, Australia). Dulbecco's modified eagle medium (DMEM), antibiotics/antimycotics, fetal calf serum (FCS), L-glutamine, dimethyl sulfoxide (DMSO, ≥99.7%) and RIPA buffer, were purchased from ThermoFisher Scientific (Paisley, UK). 3-(4,5-dimethyl-2-thiazolyl)-2,5-diphenyltetrazolium

bromide (MTT), mitomycin C (MC), Tween 20 and bovine serum albumin (BSA) were obtained from Sigma-Aldrich (Poole, UK). Fluorescent probe, Draq5™, was purchased from BioStatus (Shepshed, UK). 4% Paraformaldehyde in phosphate buffered saline (PBS) was supplied by Santa Cruz Biotechnology (Dallas, TX, USA). RNAprotect Cell Reagent was obtained from Qiagen (Manchester, UK). ECL™ Prime Detection Reagent was purchased from VWR International (Lutterworth, UK). Pan-PKC inhibitor, bisindolylmaleimide-1 (BIM-1), was obtained from Merck Millipore (Watford, UK). Primary antibodies against cytokeratin 13 (#ab133340), cytokeratin 15 (#ab52816), cytokeratin 16 (#ab76416), cytokeratin 17 (#ab109725), KRT6B (#ab154313), cyclin A2 (#ab137769), cyclin B1 (#ab32053), cyclin B2 (#ab185622), CDKN3 (#ab175393), p21 (CDKN1A, #ab109520), UBE2C (#ab125002), S100A4 (#ab124805), MRP8 (S100A8, #ab92331) and β-actin Loading Control (#ab8227) were purchased from Abcam (Cambridge, UK). Phospho-PKC (pan) primary antibody (#9371) was purchased form Cell Signaling Technology (Danvers, MA, USA). Horseradish peroxidase-conjugated secondary antibody (#P039901-2) was obtained from Dako (Ely, UK). All remaining reagents were of highest grade and either supplied by ThermoFisher Scientific or Sigma-Aldrich.

2.2. Cell culture

The immortalized human skin keratinocyte cell line (HaCaTs) was obtained from the German Cancer Research Centre (Heidelberg, Germany). HaCaTs were cultured in DMEM, supplemented with 1% antibiotics/antimycotics (100 U/mL penicillin G sodium, 100 µg/mL streptomycin sulfate and 0.25 µg/mL amphotericin B), 2 mM L-glutamine and 10% FCS [18]. HaCaTs were maintained at 37 °C in a humidified 5% CO_2/95% air atmosphere, with medium changed every 48 h.

For epoxy-tigliane-containing cultures, EBC-46 and EBC-211 were initially solubilized in DMSO at 178 mM (100 mg/mL) and 17.8 mM (10 mg/mL), respectively. Stock solutions were used to prepare further epoxy-tiglianes dilutions in DMSO, prior to dilution in 1% serum-containing DMEM at 1.78 nM-178 μM (DMSO concentrations, ≤1%). Total epoxy-tigliane solubility was subsequently confirmed by preparation of EBC-46 and EBC-211 (1.78 μM, 17.8 μM and 178 μM) in 1% serum-containing DMEM with ≤1% DMSO, centrifugation (15,000 rpm, 10 min) and subsequent analysis using a Shimadzu Prominence LC-20 HPLC System (Shimadzu, Sydney, Australia), at 249 nm, with a Halo RP-Amide 2.7 μm, 150 mm x 4.6 mm column (Hichrom, Lutterworth, UK); and acetonitrile/water solvent scheme. Profiles were compared verses linear standard curves prepared using EBC-46 and EBC-211 in DMSO (0.001-0.5 mg/mL, 1.78 μM-0.89 mM). As the solubility of both epoxy-tiglianes were determined to be ≅85% in 1% serum-containing DMEM with ≤1% DMSO, final EBC-46 and EBC-211 concentrations were adjusted to 1.51 nM-151 μM, based on a solubility factor of x0.85. Untreated control cultures were also supplemented with 1% DMSO, to discount influences on HaCaT behavior in epoxy-tigliane-treated cultures.

2.3. Cell proliferation and viability assays

HaCaTs were seeded into 96-well micro-titer plates in 10% serum-containing DMEM at 5×10^3 cells/well for 24 h, followed by incubation in serum-free DMEM for another 24 h. Serum-free media was replaced with 1% serum-containing DMEM with 0-151 μM EBC-46 and EBC-211 (6 wells/epoxy-tigliane concentration). Cultures were maintained at 37 °C in a humidified 5% CO_2/95% air atmosphere, with medium changed every 48 h. HaCaT proliferation and viability were assessed at 24 h, 72 h, 120 h and 168 h, by MTT [3-(4,5-dimethyl-2-thiazolyl)-2,5-diphenyltetrazolium bromide] assay [19]. Absorbance values were measured using a Bio-Tek Instruments Microplate Autoreader (ThermoFisher Scientific), at 540 nm. Epoxy-tigliane

effects on cell proliferation and viability were expressed as percent viable cells versus untreated controls, which were arbitrarily assigned a viability of 100%.

2.4. Cell cycle analysis

HaCaTs were seeded into 6-well plates in 10% serum-containing DMEM at 7.5×10^4 cells/well for 24 h, followed by cell cycle synchronization in serum-free DMEM for another 24 h. Serum-free media was replaced with 1% serum-containing DMEM with 0-15.1 µM EBC-46 and EBC-211 (3 wells/epoxy-tigliane concentration). Cultures were maintained at 37 °C in a humidified 5% CO_2/95% air atmosphere, for 9 h, 17 h, 26 h, 32 h, 40 h and 48 h; with 0 h analyzed at time of epoxy-tigliane treatment. At each time-point, cells were fixed with 4% paraformaldehyde in PBS and re-suspended in PBS. Fluorescent probe, Draq5™ (20 µM) [20], was added and flow cytometry performed (FACSCalibur™, BD Biosciences, Oxford, UK), per manufacturer's instructions. Data analysis was performed using FlowJo Software (BD Biosciences, Ashland, OR, USA).

2.5. Scratch wound repopulation

HaCaTs were seeded into 24-well plates in 10% serum-containing DMEM at 7.5×10^4 cells/well for 48 h, followed by incubation in serum-free DMEM for another 24 h. Serum-free DMEM was removed and scratch wounds made using sterile pipettes. Following PBS washing (×2), 1% serum-containing DMEM with 0-15.1 µM EBC-46 and EBC-211 (3 wells/epoxy-tigliane concentration) was added and cultures maintained at 37 °C in a humidified 5% CO_2/95% air atmosphere for 48 h. HaCaT migration and scratch wound repopulation were monitored by Time-Lapse Confocal Microscopy (TCS SP5 Microscope, Leica Microsystems, Milton Keynes, UK) [18]. Digital images were taken every 20 min over 48 h, using LAS AF Lite Software. Scratch wound repopulation rates were quantified using ImageJ® Software (Version 1.49,

https://imagej.nih.gov/ij/). Experiments were also repeated with sub-lethal concentrations of anti-proliferative agent, MC (1 µM), to delineate the extent to which epoxy-tigliane induced proliferative responses contributed to HaCaT scratch wound repopulation. Data were expressed as percentage wound closure at 24 h and 48 h, versus wound areas at 0 h.

2.6. Microarray analysis

HaCaTs were seeded into T-75 tissue culture flasks in 10% serum-containing DMEM at 2×10^6 cells/flask for 24 h, followed by incubation in serum-free DMEM for another 24 h. Serum-free media was replaced with 1% serum-containing DMEM with EBC-46 and EBC-211 (0 or 1.51 nM, 151 nM and 15.1 µM). Cultures were maintained at 37 °C in a humidified 5% CO_2/95% air atmosphere, for 24 h or 48 h. Culture medium was then replaced with RNAprotect Cell Reagent. RNA was extracted, amplified and labelled, using RNeasy Plus Mini Kits (Qiagen, Chadstone, Australia) and TotalPrep RNA Amplification Kits (ThermoFisher Scientific, Scoresby, Australia), according to manufacturers' instructions. Complementary RNA samples were hybridized to Human HT-12 v4 Expression BeadChips for Microarray analysis, using the Whole-Genome Gene Expression Direct Hybridization Assay System (Illumina, San Diego, CA, USA), as per manufacturer's instructions. BeadChips were scanned using the iScan System and BeadScan Software (Illumina).

Scanned data were uploaded into BeadStudio Gene Expression Module (Illumina) and imported into GeneSpring GX Expression Analysis Software (Agilent Technologies, Santa Clara, CA, USA), for normalization, filtering, statistical analysis and heatmap visualization/clustering. Data from each treatment group (n=4 replicate experiments) were grouped for combined analysis, using Ingenuity Pathway Analysis (IPA®) Software. Other databases used to identify the functional characteristics for genes of interest relevant to keratinocyte biology and re-epithelialization, included PubMed

(*http://www.ncbi.nlm.nih.gov/pubmed*) and UniProt (*https://www.uniprot.org/*). Microarray data were deposited on the Gene Expression Omnibus (GEO) database (*http://identifiers.org/geo:GSE122297*).

2.7. Western blot analysis

HaCaTs were seeded and treated with 1% serum-containing DMEM with 0-15.1 μM EBC-46 and EBC-211, as above. Cultures were harvested with RIPA buffer (1 mL), containing Complete Protease Inhibitor Cocktail Tablets (Roche, Burgess Hill, UK). Protein samples (10 μg) were separated by sodium dodecyl sulfate-polyacrylamide gel electrophoresis (SDS-PAGE) on pre-formed 4-15% TGX™ gels (Mini-Protean® Tetra Cell System; Bio-Rad, Hemel Hempstead, UK). Gels were electroblotted onto polyvinylidene difluoride (PVDF) membranes (Hybond™-P, ThermoFisher Scientific), except for phospho-PKC (pan) blots where nitrocellulose membranes (ThermoFisher Scientific) were used. Electroblotting was performed using a Mini Trans-Blot® Electrophoretic Transfer Cell (Bio-Rad), as per manufacturer's instructions.

PVDF membranes were blocked with 5% semi-skimmed milk/1% Tween 20 in Tris-buffered saline (TBS) for 1 h at room temperature, followed by primary antibody incubation in 5% semi-skimmed milk/1% Tween 20, for 1 h at room temperature or 4°C overnight. Nitrocellulose membranes were blocked with 5% BSA/1% Tween 20 in TBS for 1 h at room temperature, followed by primary antibody incubation in 5% BSA/1% Tween 20/TBS, for 1 h at room temperature or 4°C overnight. All membranes were washed (×3) in 1% Tween 20/TBS and incubated with horseradish peroxidase-conjugated secondary antibody, in 5% semi-skimmed milk/1% Tween 20/TBS for 1 h at room temperature. Membranes were washed (×3) as above, followed by additional 5 min washes (×1) in TBS. Membranes were incubated in ECL™ Prime Detection Reagent and autoradiographic films (Hyperfilm™-ECL, ThermoFisher

Scientific) developed, per manufacturer's instructions. Immunoblot images were captured and densitometric analysis performed using ImageJ® Software, with untreated controls at each respective time-point representing 1.0-fold.

2.8. MMP activity quantification

HaCaTs were seeded and treated with 1% serum-containing DMEM with 0-15.1 µM EBC-46 and EBC-211, as above. Cultures were maintained at 37 °C in a humidified 5% CO_2/95% air atmosphere, for 24 h or 48 h. Culture media was collected and MMP-1, MMP-7 and MMP-10 activities quantified using SensoLyte® 520 Activity Assays (Cambridge Bioscience, Cambridge, UK), according to manufacturer's instructions at 490 nm/520 nm, as above. Activities were expressed as relative fluorescence units (RFU).

2.9. Cytokine and chemokine level quantification

HaCaTs were seeded and treated with 1% serum-containing DMEM with 0-15.1 µM EBC-46 and EBC-211, as above. Cultures were maintained at 37 °C in a humidified 5% CO_2/95% air atmosphere, for 24 h or 48 h. Culture media was collected and epoxy-tigliane effects on IL-6, IL-8, CCL5 and CXCL10 levels quantified using Quantikine® ELISAs (R&D Systems, Abingdon, UK), as per manufacturer's instructions. Absorbance values were measured at 450 nm as above, with data expressed as pg/mL.

2.10. PKC involvement in epoxy-tigliane wound healing responses

HaCaTs were seeded, as above. HaCaTs were subsequently incubated in 1% serum-containing DMEM with EBC-46 and EBC-211 (0 or 1.51 nM, 151 nM and 15.1 µM) ± sub-lethal concentrations of pan-PKC inhibitor, BIM-1 (1 µM, solubilized in DMSO), followed by assessment of HaCaT proliferation at 24 h, 48 h and 72 h (MTT assay) and HaCaT

migration/wound repopulation at 24 h and 48 h (Time-Lapse Microscopy), as above. PKC effects on keratin (KRT17) and cell cycle/proliferation-associated (cyclin B1, CDKN1A) protein levels, with EBC-46 and EBC-211 (1.51 nM, 151 nM and 15.1 μM), were confirmed by Western blot analysis (10 μg protein samples) as above, ± BIM-1 (1 μM). PKC effects on MMP-1, MMP-7 and MMP-10 activities with EBC-46 and EBC-211 (1.51 nM, 151 nM and 15.1 μM), were confirmed by activity assays as above, ± BIM-1 (1 μM).

To confirm PKC phosphorylation and activation following epoxy-tigliane treatment, HaCaTs were seeded into T-75 tissue culture flasks and treated with EBC-46 and EBC-211 (0 or 1.51 nM, 151 nM and 15.1 μM) for 0 h, 30 min, 1 h, 3 h, 6 h and 24 h. Cell extracts were harvested and protein samples (10 μg) separated and electroblotted, as above. Membranes were blocked in 5% BSA/1% Tween 20 in TBS and immuno-probed with phospho-PKC (pan) primary antibody in 5% BSA/1% Tween 20/TBS, at 4°C overnight. Protein loading confirmation, secondary antibody incubations, protein detection and image capture, were performed as above.

2.11. Statistical analysis

Microarrays were performed on n=4 replicate experiments. All other experiments were performed on n=3 independent occasions. Data were expressed as mean ± standard error of the mean (SEM). Proliferation, wound repopulation, MMP activity and ELISA data were analyzed by one-way ANOVA with post-Tukey test. Cell cycle data were analyzed using one-way ANOVA with Dunnett Multiple Comparisons test. Western blot densitometry data were analyzed using unpaired Student's t tests. Microarray data were analyzed using unpaired Student's t tests, with Benjamini/Hochberg multiple test correction. Significance were considered at $p<0.05$. Tables summarizing the statistically significant differences identified in

each experiment following epoxy-tigliane treatment versus untreated controls; are accessible via the Supplementary Dataset [21].

3. Results

3.1. Epoxy-tiglianes stimulate keratinocyte cell cycle progression and proliferation

Initial studies determined whether EBC-46 and EBC-211 (1.51 nM-151 µM) stimulated HaCaT proliferation *in vitro* versus untreated controls, by MTT assay. Although both epoxy-tiglianes induced significant cytotoxicity at 151 µM ($p<0.001$ at all time-points), stimulated proliferative responses were evident with 1.51 nM-15.1 µM EBC-46 and EBC-211 (Fig. 1B & C). Most profound proliferation effects were observed at 72 h across all epoxy-tigliane concentrations ($p<0.001$). Enhanced proliferative responses were also apparent at 24 h (1.51 nM, $p<0.01$), 120 h (1.51 nM and 1.51 µM EBC-46; 1.51-151 nM EBC-211, $p<0.001$); and 168 h (1.51 nM and 151 nM-15.1 µM EBC-46; 1.51 nM-151 µM EBC-211, $p<0.001$-0.05).

Based on these stimulated HaCaT proliferative responses, flow cytometry confirmed epoxy-tigliane effects on HaCaT cell cycle progression. Following cell cycle synchronization by serum starvation (0 h), no significant differences were identified between EBC-46-treated and untreated controls at 9 h ($p>0.05$, [21]). However, at 17 h, 26 h, 32 h and 40 h, significant cycle progression through G0/G1-S and S-G2/M phases was evident versus controls at all EBC-46 concentrations ($p<0.01$-0.05, Fig. 1D at 40 h and at 17 h, 26 h and 32 h, [21]), corroborating significantly increased proliferative responses between 24-72 h (Fig. 1B). Only marginal increases in cell cycle progression were evident at 48 h ($p<0.05$, [21]). EBC-211-treated HaCaTs demonstrated similarly increased cell cycle progression versus untreated controls, albeit with less dramatic cell cycle acceleration than EBC-46. Although no significant differences were observed at 0 h, 9 h or 17 h ($p>0.05$, [21]), significant cell cycle progression through G0/G1-S and S-G2/M phases was evident at 26 h, 32 h, 40 h and 48 h versus controls, at all EBC-211 concentrations ($p<0.01$-0.05, Fig. 1E at 40 h and 26 h, 32 h and 48 h, [21]).

3.2. Epoxy-tiglianes stimulate keratinocyte scratch wound repopulation

We next assessed EBC-46 and EBC-211 (1.51 nM-15.1 µM) effects on HaCaT migration and wound repopulation using automated *in vitro* scratch wounds. Time-Lapse images and ImageJ® analysis showed HaCaT migration and re-population of denuded wound spaces, with untreated controls promoting ≈50% closure over 48 h (Fig. 2A & B and 2C & D for EBC-46 and EBC-211, respectively). Although wound closure was not significantly different with most EBC-46-treated HaCaTs (15.1 nM-15.1 µM) versus controls at 24 h ($p>0.05$, Fig. 2A & B and Supplementary Video S1 online), 1.51 nM EBC-46 did significantly enhance closure at 24 h ($p<0.01$, Fig. 2A & B and Supplementary Video S2 online). At 48 h, significantly increased closure was further evident at 1.51-151 nM EBC-46 versus controls ($p<0.001$-0.01), with almost complete closure observed due to enhanced wound edge HaCaT migration and increased bursts of proliferation behind the migrating front between 24-48 h (Fig. 2A & B and Supplementary Videos S1 & S2 online for untreated and 1.51 nM EBC-46 treated HaCaTs respectively; Supplementary Videos for 15.1-151 nM EBC-46 treated HaCaTs, [21]). However, higher EBC-46 concentrations (1.51-15.1 µM) demonstrated no significant differences in wound closure rates ($p>0.05$, Fig. 2A & B and Supplementary Videos [21]).

Similar responses were evident with EBC-211 over a wider concentration range (Fig. 2C & D and Supplementary Videos S3 & S4 online for untreated and 1.51 nM EBC-211 treated HaCaTs; Supplementary Videos for 15.1 nM-15.1 µM EBC-211 treated HaCaTs, [21]), with increased wound edge HaCaT migration and adjacent cell proliferation resulting in significantly enhanced wound closure with 1.51-151 nM EBC-211 at 24 h ($p<0.001$-0.05) and 1.51 nM-15.1 µM EBC-211 at 48 h ($p<0.001$-0.05). This was particularly apparent at 1.51-151 nM EBC-211, where almost complete wound closure was shown.

3.3. Epoxy-tigliane stimulation of wound repopulation independently of proliferation

As wound repopulation is dependent on the induction of both migratory and proliferative responses, we next ascertained the extent to which the significantly induced proliferative responses in epoxy-tigliane-treated HaCaTs contributed to enhance scratch wound repopulation using anti-proliferative agent, MC. Time-Lapse Microscopy and ImageJ® analysis over 48 h confirmed significant EBC-46 (1.51 nM-1.51 µM) stimulation of wound closure versus untreated controls (Fig. 3A and Supplementary Videos, [21]), even with MC. At 24 h, only 1.51 nM EBC-46 induced significant closure with MC versus controls, both with and without MC ($p<0.001$). At 48 h, significantly enhanced closure was further evident with 1.51 nM-1.51 µM EBC-46 and MC ($p<0.001$-0.05), compared to controls with and without MC (Fig. 3A and Supplementary Videos, [21]). Similar findings were obtained with EBC-211, with increased wound closure following treatment with 1.51 nM-1.51 µM EBC-211 and MC, versus controls with and without MC (Fig. 3B and Supplementary Videos, [21]). Wound closure was significantly increased with 1.51-151 nM EBC-211 and MC at 24 h ($p<0.001$-0.01), with further enhancements at 48 h with 1.51 nM-1.51 µM EBC-211 and MC ($p<0.001$), compared to controls with and without MC.

3.4. Epoxy-tiglianes alter keratinocyte gene expression profiles to stimulate proliferation and migration

Having demonstrated clear epoxy-tigliane stimulatory effects on HaCaT proliferation and migration/wound repopulation responses, we next performed global gene expression analysis to explain these findings. EBC-46 and EBC-211 (1.51 nM, 151 nM and 15.1 µM) effects on HaCaT gene expression were assessed at 24 h and 48 h. Expression analysis identified numerous genes to be differentially expressed by EBC-46 and EBC-211 versus untreated controls, particularly at 48 h. Hierarchical clustering heatmaps (Fig. 4A) demonstrated that for

most genes, similar expression changes were induced irrespective of epoxy-tigliane or concentration. Due to the large numbers identified, only genes differentially expressed ≥2-fold were analysed further. Differentially expressed genes were classified with particular relevance to keratinocyte wound healing responses, potentially contributing to stimulatory epoxy-tigliane effects on keratinocyte proliferation and migration. These included keratin (KRT); DNA synthesis/replication; cell cycle, proliferation and apoptosis; adhesion/migration; differentiation; proteinase; and cytokine/chemokine genes (Tables presenting these differentially expressed gene categories are available, [21]). See GEO database (GSE122297) for full dataset.

3.5. Epoxy-tiglianes modulate keratin protein levels to enhance keratinocyte proliferation and migration

In line with the key roles that KRTs play in keratinocyte biology and re-epithelialization [5,22], the significant up-regulation of KRT9, KRT13, KRT15 and down-regulation of KRT6B, KRT16, KRT17 by epoxy-tiglianes were particularly striking. Concurrent with expression findings, Western blot validation showed limited increases in KRT13 protein levels versus untreated controls with EBC-46 and EBC-211 at 24 h ($p>0.05$, [21]), although further increases in KRT13 were shown at 48 h with 1.51 nM-15.1 µM EBC-46 [21] and 151 nM EBC-211 ($p<0.05$, Fig. 4B). Although no significant decrease in KRT15 detection levels were identified with EBC-46 ($p>0.05$, [21]), a significant decrease in KRT15 was evident with 15.1 µM EBC-211 at 24 h ($p<0.05$, Fig. 4C), but not 48 h [21]. However, despite suggested KRT16, KRT17 and KRT6B down-regulation by expression profiling analysis, no consistent decreases in KRT16, KRT17 or KRT6B protein levels were evident following epoxy-tigliane treatments ($p>0.05$, [21]).

3.6. Epoxy-tiglianes influence cell cycle-related proteins to enhance keratinocyte proliferation and migration

A number of significantly up-regulated (cyclin A2, cyclin B1, cyclin B2, CDKN3 and UBE2C) and down-regulated (CDKN1A) cell cycle-related genes, were also assessed at the protein level. Although Western blotting demonstrated equivalent cyclin A2 detection with EBC-46 and EBC-211 versus untreated controls at 24 h [21], in line with the profiling findings, significantly increased cyclin A2 protein expression (Fig. 5A) were detectable with 15.1 nM and 1.51 µM EBC-46 ($p<0.05$), at 48h; but not with EBC-211 ($p>0.05$, [21]). Cyclin B1 also exhibited increased levels of detectable protein expression with 151 nM-15.1 µM EBC-46 (Fig. 5B), at 24 h only ($p<0.001$-0.01). Cyclin B2 protein levels were significantly increased by EBC-46 (Fig. 5C) at 24 h (15.1 µM, $p<0.05$) and 48 h (151 nM-15.1 µM, $p<0.05$). Although non-significant increases in cyclin B1 protein levels were consistently detectable with EBC-211 at 24 h and 48 h [21], significantly increased cyclin B2 detection was apparent with 1.51 nM EBC-211 ($p<0.05$), at 48 h only (Fig. 5D). CDKN3 and UBE2C detection exhibited no discernible differences with EBC-46 or EBC-211 at 24 h or 48 h ($p>0.05$, [21]). In contrast, cell cycle inhibitor, CDKN1A, showed significantly reduced levels at 24 h (Fig. 5E), following treatment with 1.51 nM-15.1 µM EBC-46 and EBC-211 ($p<0.001$), although reductions were less apparent at 48 h ($p>0.05$, [21]).

3.7. Epoxy-tiglianes increase matrix metalloproteinase activities in keratinocytes

As matrix metalloproteinases (MMPs) have prominent roles in mediating keratinocyte detachment from the basal lamina and migration across the wound extracellular matrix (ECM) [5], the epoxy-tigliane-induced up-regulation of MMP-1, MMP-7 and MMP-10 were noteworthy, given the absence of up-regulated MMP inhibitor expression [21] (GEO database, GSE122297). Activity assays confirmed increased MMP expression following epoxy-tigliane

treatments (Fig. 6A), with significantly elevated MMP-1 activities with 1.51 nM-1.51 µM EBC-211 at 24 h ($p<0.001$); and both epoxy-tiglianes at 48h (1.51 nM-15.1 µM, $p<0.001$-0.05). Similarly, MMP-7 activities (Fig. 6B) were significantly increased by 1.51-151 nM EBC-46 ($p<0.01$-0.05) and 1.51 nM-1.51 µM EBC-211 ($p<0.01$-0.05) at 24 h; in addition to 1.51-15.1 nM EBC-46 ($p<0.001$-0.05) and 1.51 nM-1.51 µM EBC-211 ($p<0.001$-0.05), at 48 h. Although EBC-46 induced no significant increases in MMP-10 activities ($p>0.05$, Fig. 6C), significantly increased MMP-10 activities were shown with 1.51 nM-15.1 µM EBC-211 at 24h and 48h ($p<0.001$-0.01).

3.8. Epoxy-tiglianes regulate S100 protein expression in keratinocytes

As highlighted by the expression profiling analyses [21] (GEO database, GSE122297), differentially expressed S100 proteins also possess influential roles on keratinocyte proliferation and migration [23,24]. Western blotting demonstrated no significant differences in S100A4 protein levels with 1.51 nM-15.1 µM EBC-211 treatment versus untreated controls at 24 h or 48 h ($p>0.05$, [21]), although significant increases in S100A4 were detectable at 24 h (Fig. 6D) with 15.1 µM EBC-46 ($p<0.05$). Despite S100A8 being undetectable in control and epoxy-tigliane-treated cultures at 24 h [21], significantly decreased S100A8 protein levels were determined at 48 h versus untreated controls (Fig. 6E) with 1.51 nM-15.1 µM EBC-46 ($p<0.001$); and with 151 nM and 15.1 µM EBC-211 ($p<0.05$).

3.9. Epoxy-tiglianes down-regulate established cytokine/chemokine agonists of keratinocyte proliferation and migration

Epidermal keratinocyte functions, including migratory and proliferative responses, are well-established to be regulated by various cytokines and chemokines [25]. However, both epoxy-tiglianes significantly down-regulated the expression of cytokines, including interleukin (IL)-

1α, IL-6, IL-8 and tumour necrosis factor-α (TNF-α); and chemokine (C-C motif) ligands, (CCL)2, CCL5 and chemokine (C-X-C motif) ligands, (CXCL)1 and CXCL10 [21] (GEO database, GSE122297). Epoxy-tigliane down-regulation of selected cytokines and chemokines were verified by ELISA. Although EBC-46 induced no significant changes in IL-6 levels at 24 h ($p>0.05$, Fig. 7A), 1.51 nM-15.1 μM EBC-46 significantly decreased IL-6 levels at 48 h ($p<0.001$-0.01). Despite a significant increase in IL-6 levels with 15.1 μM EBC-211 at 24 h ($p<0.05$, Fig. 7A), significant decreased IL-6 levels were also evident with 1.51 nM-15.1 μM EBC-211 versus untreated controls at 48 h ($p<0.001$). Although IL-8 levels were significantly increased by 15.1 nM-15.1 μM EBC-46 ($p<0.001$-0.01) and 151 nM-15.1 μM EBC-211 ($p<0.001$-0.05) at 24 h (Fig. 7B), significant decreases in IL-8 levels were detected with 1.51 nM and 15.1 μM EBC-46 ($p<0.01$-0.05) and 1.51 nM-15.1 μM EBC-211 ($p<0.001$-0.05) at 48 h. EBC-46 and EBC-211 (1.51 nM-15.1 μM) were further demonstrated to significantly decrease CCL5 levels versus untreated controls (Fig. 7C), both at 24 h ($p<0.001$-0.01 for EBC-46, $p<0.001$ for EBC-211) and 48 h ($p<0.001$ for both EBC-46 and EBC-211). Similar profiles were apparent with CXCL10 (Fig. 7D), with significant reductions in CXCL10 levels with 1.51 nM-15.1 μM EBC-46 and EBC-211 at 24 h ($p<0.001$-0.01 for EBC-46; $p<0.001$ for EBC-211) and 48 h ($p<0.001$ for both EBC-46 and EBC-211).

3.10. Epoxy-tiglianes promote keratinocyte proliferation and migration via PKC activation

The predominant down-regulation of such cytokines and chemokines implied that epoxy-tigliane stimulation of HaCaT proliferation and migration were not facilitated via such autocrine mechanisms. As previous work identified that the anti-cancer effects of EBC-46 are induced by PKC activation [1], we next established whether PKC activation was also responsible for the changes identified above, leading to enhanced HaCaT proliferative and migratory responses. Studies assessed whether the stimulatory effects of EBC-46 and EBC-

211 on HaCaT proliferation and scratch wound repopulation were abrogated by the pharmacological inhibition of PKC activation by pan-PKC inhibitor, BIM-1. Although both epoxy-tiglianes induced significant HaCaT proliferation at 1.51 nM, 151 nM and 15.1 µM concentrations versus untreated controls, in line with previous findings, these responses were significantly abrogated by BIM-1 at 24 h, 48 h and 72 h post-treatment ($p<0.001$, Fig. 8A & B). The significantly enhanced scratch wound closure induced by EBC-46 versus untreated controls, were also significantly inhibited by BIM-1 at 24 h (1.51 nM, $p<0.001$) and 48 h (151 nM and 15.1 µM, $p<0.001$, Fig. 8C & D and Supplementary Videos, [21]). Similarly, BIM-1 significantly inhibited wound closure induced by EBC-211 at 24 h (1.51 nM and 15.1 µM, $p<0.001$) and 48 h (1.51 nM-15.1 µM, $p<0.001$, Fig. 8E & F and Supplementary Videos, [21]).

3.11. Epoxy-tiglianes modulate keratin, cell cycle-related protein and matrix metalloproteinase levels via PKC activation

We next evaluated BIM-1 effects on the differential expression of selected KRT, cell cycle and MMP proteins, following treatment with EBC-46 and EBC-211. BIM-1 treatment significantly increased KRT17 protein levels induced by 15.1 µM EBC-46 ($p<0.01$) and 151 nM EBC-211 ($p<0.05$), at 24 h (Fig. 9A). BIM-1 had no significant effects on the EBC-46 induced protein levels of cyclin B1 ($p>0.05$, [21]). However, a significant increase in cyclin B1 levels was evident after 48 h treatment with 15.1 µM EBC-211 ($p<0.01$, Fig. 9B). BIM-1 was further demonstrated to abrogate the epoxy-tigliane-induced down-regulation of CDKN1A, with significant increases in CDKN1A detection following 15.1 µM EBC-46 treatment at 24 h ($p<0.01$, Fig. 9C) and 151 nM EBC-46 at 48 h ($p<0.05$); in addition to significant CDKN1A increases with 1.51 nM EBC-211 at 48 h ($p<0.05$, Fig. 9D). Furthermore, BIM-1 significantly inhibited epoxy-tigliane-induced increases in the activities of MMP-1 (1.51 nM-15.1 µM,

$p<0.001$, Fig. 9E), MMP-7 (1.51 nM and 151 nM EBC-46; 1.51 nM-15.1 µM EBC-211, $p<0.001$-0.05, Fig. 9F); and MMP-10 (1.51 nM-15.1 µM, $p<0.001$, Fig. 9G), at 48 h.

Western blot detection of pan-PKC phosphorylation and activation further showed that compared to untreated controls (Fig. 10A), EBC-46 induced PKC phosphorylation, with a dose-dependent response evident at 1 h, with the greatest increase in phosphorylation induced at 15.1 µM. Following 3 h treatment, 151 nM EBC-46 showed the greatest induction of PKC phosphorylation. The dose-dependent induction was again evident at 6 h and 24 h, with 15.1 µM EBC-46 showing the greatest response. EBC-211 also promoted rapid phosphorylation at 15.1 µM at 30 min and 1 h (Fig. 10B). Following a decline in PKC phosphorylation at 3 h, induction was evident at 6 h with 1.51 nM and 151 nM EBC-211, although PKC phosphorylation returned to baseline levels at 24 h.

4. Discussion

This study provides previously unreported insights into how novel epoxy-tiglianes promote keratinocyte wound healing responses, in line with the accelerated re-epithelialization and wound closure *in vivo*, post-tumor destruction [1-3]. Epithelial integrity is maintained by keratinocytes that switch from basal proliferative states to differentiated states, upon migration through the epidermis [5]. In acute healing skin wounds, disassembled cell-cell and cell-matrix interactions initiate keratinocyte migration from the wound edge across denuded areas, whereas keratinocytes behind the migrating front proliferate. However, during non-healing chronic skin wounds, mitotically active keratinocytes are localized within the supra-basal layers of the epithelium due to c-myc activation and overexpression, which impairs healing [7]. Furthermore, as the epidermal margins of chronic wounds are highly proliferative, keratinocytes exhibit a non-migratory phenotype, partly through the failed disruption of cell-

cell and cell-matrix interactions [9-11]. Consequently, these events attenuate re-epithelialization and the re-establishment of barrier function.

This study demonstrated that both EBC-46 and EBC-211 induced significant HaCaT proliferation, with concomitant accelerated cell cycle transitions between G1/S and S/G2 phases. Coupled with stimulated proliferation were the abilities of EBC-46 and EBC-211 to enhance HaCaT migratory and wound repopulation responses, even with MC-inhibited proliferation, suggesting that epoxy-tiglianes can promote keratinocyte migration and wound repopulation independently of proliferation. Based on these findings, epoxy-tiglianes appear to promote keratinocyte hyper-proliferation. However, as epoxy-tiglianes also enhanced keratinocyte migration and wound repopulation over equivalent time frames, this implies that epoxy-tigliane hyper-proliferative responses are shorter than the prolonged hyper-proliferation associated with chronic wounds. Furthermore, increased bursts of proliferative activity were evident behind wound edge keratinocytes in repopulation time-lapse videos following epoxy-tigliane treatment, akin to proliferative bursts occurring behind migrating keratinocytes in acute wound margins [26]. Therefore, similar events may be induced by epoxy-tiglianes *in vivo* permitting re-epithelialization, with keratinocyte differentiation presumably resumed upon epidermal barrier restoration [27]. Indeed, accelerated keratinocyte proliferative/migratory responses and rapid re-epithelialization are hallmarks of highly regenerative tissues, such as early-gestational fetal skin and oral mucosa [28,29].

Expression profiling and validation analyses demonstrated that EBC-46 and EBC-211 collectively induce gene expression changes driving DNA synthesis/replication, cell cycle progression, proliferation and migration to facilitate enhanced wound re-epithelialization; at the expense of genes associated with apoptosis and keratinocyte differentiation. Of these, the KRTs were particularly prominent, given the pivotal roles of keratin heterodimers and intermediate filaments in regulating keratinocyte functions and epithelial integrity [22]. Up-regulated

KRT13 and KRT15 were particularly interesting, as these are not typically found in adult skin epithelia but are common in supra-basal layers of non-keratinized, oral mucosal and fetal epithelia respectively, where these promote rapid re-epithelialization [29,30]. KRT13 up-regulation is also associated with alternative differentiation and the re-induction of embryonic epidermal regeneration [31]. KRT15 is present in epidermal stem cells and basal keratinocytes of stratified epithelia, where it stimulates keratinocyte proliferation, although its expression declines during terminal differentiation [32].

Although KRT6B, KRT16 and KRT17 are common in stratified epithelia and absent in uninjured tissue, their down-regulation was unexpected considering the extent of HaCaT proliferation and migration induced by epoxy-tiglianes. Type I/II intermediate filament partners, KRT6, KRT16 and KRT17, are markers of decreased desmosome adhesion, increased contractility and activated hyper-proliferative/migratory responses in wound edge keratinocytes during re-epithelialization [25,33]. However, KRT16 protein is restricted to post-mitotic keratinocytes, whilst over-expression inhibits keratinocyte proliferation, migration and re-epithelialization [34]. Down-regulation of KRT6 and its heterodimer, KRT16, also enhances keratinocyte migration and re-epithelialization [35,36]; although KRT17 down-regulation inhibits these responses [37]. Therefore, despite our findings being partly counterintuitive to the roles these KRTs play post-injury, such studies collectively support the epoxy-tigliane manipulation of KRT expression to promote keratinocyte proliferation and migration.

In addition to KRTs, epoxy-tiglianes particularly influenced the expression of a multitude of genes to promote HaCaT proliferation. In line with epoxy-tiglianes stimulating G0/G1-S and S-G2/M transitions, these included up-regulated cyclins A2, B1 and B2 which promote G2/M transition, while cyclin A2 also controls G1-S transition [38]. Concomitant with cyclin up-regulation were the differentially regulated cyclin-dependent inhibitors, CDKN3 and CDKN1A. Up-regulated CDKN3 regulates normal mitosis and G1-S transition by arresting G1

phase [39], whilst down-regulated CDKN1A attenuates cyclin complex formation with cyclin-dependent protein kinases, inhibiting G1-S transition [40]. Other up-regulated genes with prominent roles in positively mediating various aspects of DNA synthesis/replication, cell cycle transition, mitosis, cytokinesis and proliferation, included mini-chromosome maintenance proteins, aurora kinases, cell division cycle and centromere proteins, kinesins, GINS2 and UBE2C (GEO database, GSE122297) [21,41-46]. In contrast, pro-apoptosis-related genes, such as caspases and TNF superfamily members, were down-regulated by epoxy-tiglianes [21,47,48].

Differential S100 protein expression by epoxy-tiglianes would further influence proliferation and migration, as up-regulated S100A4 enhances cell cycle transition, keratinocyte hyper-proliferation and motility [23,24]. In contrast, down-regulated S100A7, S100A8 and S100A9 would attenuate keratinocyte differentiation and promote proliferation/migration [49,50]. The significantly enhanced HaCaT migratory responses induced by epoxy-tiglianes would further potentially be stimulated through AGR2 up-regulation [21,51], although other pro-migratory mediators, such as LCN2, were down-regulated [21,52]. In further support of augmented HaCaT proliferative and migratory responses, as opposed to differentiation, numerous established keratinocyte differentiation markers were down-regulated by epoxy-tiglianes, including ANGPTL4, CLCA2, FABP5, LAMP3 and RARRES3 (GEO database, GSE122297) [21,53-57].

To facilitate keratinocyte migration across underlying matrix during re-epithelialization, keratinocytes disassemble cell-cell and cell-ECM interactions. Epoxy-tiglianes up-regulated MMP-1, MMP-7 and MMP-10, with no effects on MMP inhibitors, potentially enhancing keratinocyte migration and re-epithelialization via the degradation of basement membranes and underlying dermal matrices [58-60]. Despite enhanced HaCaT proliferative and migratory responses by epoxy-tiglianes, many serine proteases and their

inhibitors commonly associated with hyper-proliferative keratinocytes, such as PLAU, PI3 and SERPINs; were down-regulated by epoxy-tiglianes (GEO database, GSE122297) [21,61-66].

Numerous cytokines and chemokines play critical roles in activating keratinocyte proliferation and migration during re-epithelialization [25]. However, many cytokine and chemokine agonists of keratinocyte proliferation and migration were down-regulated by epoxy-tiglianes, possibly as a consequence of altered KRT expression [36], implying that these do not mediate stimulated keratinocyte responses. Previous studies have identified that epoxy-tiglianes possess potent PKC activation capabilities, particularly the classical PKC isoforms (α, βI, βII and γ) [1]. PKCs are serine/threonine kinases ascribed numerous roles in regulating keratinocyte functions, with the calcium-/diacylglycerol-dependent, classical PKCs having opposing proliferative, migratory and differentiation effects [67]. In agreement, both epoxy-tiglianes induced PKC activation, with selected differentially expressed genes and stimulated keratinocyte proliferative/migratory responses identified to be PKC-dependent. However, although epoxy-tigliane bioactivities showed similar gene expression profiles and wound healing responses, differences in PKC activation potency were identified. Such subtle differences in PKC phosphorylation, keratinocyte gene expression and responsiveness between epoxy-tigliane analogues and concentrations, are likely consequences of differences in PKC isoform expression, distribution, translocation and activity, potentially leading to dose-independent or biphasic effects on cellular activities; as established with other PKC activators [67]. Indeed, short-term exposure or low PKC activator concentrations are recognized to promote rapid PKC intracellular translocation and activation, whereas further exposure or higher activator concentrations induce catalytic PKC domain release from the inhibitory PKC pseudo-substrate domain, resulting in constitutive activation. Although prolonged exposure can down-regulate PKC activity via catalytic PKC domain proteolysis, PKCα is resistant to such degradation during sustained stimulation [68]. Therefore, the prolonged PKC

phosphorylation and activation induced by epoxy-tiglianes, particularly at higher concentrations, appear responsible for changes in the expression of downstream targets, such as KRTs, cyclins and MMPs; leading to enhanced keratinocyte wound healing responses.

PKCα is the most abundant isoform in the epidermis, localised to supra-basal layers. PKCα is anti-proliferative and stimulatory to keratinocyte differentiation/wound re-epithelialization. In contrast, PKCγ is undetectable in keratinocytes [69], whilst PKCβ promotes keratinocyte proliferation and inhibits differentiation [70,71]; although both PKCα and PKCβII facilitate keratinocyte motility [11,72]. This suggests that epoxy-tigliane enhancement of keratinocyte proliferation, migration and re-epithelialization are principally mediated by PKCα and PKCβ isoforms. Unlike acute healing wounds, PKCα activation and keratinocyte migration are impaired in non-healing, chronic wounds [11]. However, as type I/II intermediate filament partners, KRT6 and KRT17, promote PKCα activation and keratinocyte migration [33]; KRT6 and KRT17 down-regulation by epoxy-tiglianes implies that enhanced keratinocyte migration occurs via alternative mechanisms. Consequently, although we anticipate that both PKCα and PKCβ are key contributors to enhanced keratinocyte proliferation and migration by epoxy-tiglianes, further studies will delineate the precise involvement of specific PKC isoforms in regulating epoxy-tigliane wound healing responses and other downstream cell signalling pathways involved in mediating these responses. Furthermore, as EBC-46 and EBC-211 comprise some of the >20 different natural and semi-synthetic epoxy-tigliane analogues now available, we are also investigating their structure-functional relationships amongst this broader group of compounds relevant to PKC activity, keratinocyte wound healing responses and re-epithelialization, with the ultimate objective of selecting lead candidate(s) for future development as wound healing pharmaceuticals.

In summary, this study has demonstrated that epoxy-tigliane activation of PKCs induces the multi-faceted modulation of keratinocyte gene expression, which collectively drives the

stimulation of proliferation and migratory responses; thereby explaining the enhanced wound re-epithelialization observed in epoxy-tigliane-treated skin, post-tumor destruction. As existing therapies are generally inadequate, such findings highlight the potential and further development of epoxy-tiglianes as a novel class of topical therapeutics for other clinical situations associated with impaired re-epithelialization, such as non-healing skin wounds.

Conflicts of Interest

This work was conducted with financial assistance from QBiotics Group and the Cardiff Institute of Tissue Engineering and Repair (CITER). P.R. and V.G. are employees and have ownership interests in QBiotics Group. R.M., R.S., R.L.M., P.R., V.G., G.M.B. and QBiotics Group have filed patents on the work presented in this manuscript. R.A.H. and R.J.E. have no competing interests to declare.

Acknowledgments

R.L.M. acknowledges PhD Studentship and Postdoctoral research funding from QBiotics Group, supported by funding from the Cardiff Institute of Tissue Engineering and Repair (CITER).

Author Contributions

R.L.M. and J.P.J. performed the experiments and data analysis. R.L.M. prepared the figures for the manuscript. R.M. wrote the manuscript. R.M., R.S., P.R., J.P.J. V.G., G.M.B., R.A.H., R.J.E. and R.L.M. contributed to experimental design and manuscript revision. P.R. and V.G. funded this study.

References

[1] G.M. Boyle, M.M. D'Souza, C.J. Pierce, R.A. Adams, A.S. Cantor, J.P. Johns, L. Maslovskaya, V.A. Gordon, P.W. Reddell, P.G. Parsons, Intra-lesional injection of the novel PKC activator EBC-46 rapidly ablates tumors in mouse models, PLoS One 9 (10) (2014) e108887.

[2] C.M.E. Barnett, N. Broit, P.Y. Yap, J.K. Cullen, P.G. Parsons, B.J. Panizza, G.M. Boyle, Optimising intr atumoral treatment of head and neck squamous cell carcinoma models with the diterpene ester, Tigilanol tiglate, Invest. New Drugs 37 (1) (2019) 1-8.

[3] J. Miller, J. Campbell, A. Blum, P. Reddell, V. Gordon, P. Schmidt, S. Lowden, Dose characterization of the investigational anticancer drug tigilanol tiglate (EBC-46) in the local treatment of canine mast cell tumors, Front. Vet Sci. 2019 (2019) 00106.

[4] B.J. Panizza, P. de Souza, A. Cooper, A. Roohullah, C.S. Karapetis, J.D. Lickliter, Phase I dose-escalation study to determine the safety, tolerability, preliminary efficacy and pharmacokinetics of an intratumoral injection of tigilanol tiglate (EBC-46), EBioMedicine 50 (2019) 433-441.

[5] I. Pastar, O. Stojadinovic, N.C. Yin, H. Ramirez, A.G. Nusbaum, A. Sawaya, S.B. Patel, L. Khalid, R.R. Isseroff, M. Tomic-Canic, Epithelialization in wound healing: A comprehensive review, Adv. Wound Care 3 (7) (2014) 445-464.

[6] T.C. Wikramanayake, O. Stojadinovic, M. Tomic-Canic, Epidermal differentiation in barrier maintenance and wound healing, Adv. Wound Care 3 (3) (2014) 272-280.

[7] O. Stojadinovic, H. Brem, C. Vouthounis, B. Lee, J. Fallon, M. Stallcup, A. Merchant, R.D. Galiano, M. Tomic-Canic, Molecular pathogenesis of chronic wounds: The role of β-catenin and c-myc in the inhibition of epithelialization and wound healing, Am. J. Pathol. 167 (1) (2005) 59-69.

[8] O. Stojadinovic, I. Pastar, S. Vukelic, M.G. Mahoney, D. Brennan, A. Krzyzanowska, M. Golinko, H. Brem, M. Tomic-Canic, Deregulation of keratinocyte differentiation and activation: A hallmark of venous ulcers, J. Cell. Mol. Med. 12 (6B) (2008) 2675-2690.

[9] M.L. Usui, J.N. Mansbridge, W.G. Carter, M. Fujita, J.E. Olerud, Keratinocyte migration, proliferation and differentiation in chronic ulcers from patients with diabetes and normal wounds, J. Histochem. Cytochem. 56 (7) (2008) 687-696.

[10] C.C. Lan, C.S. Wu, H.Y. Kuo, S.M. Huang, G.S. Chen, Hyperglycaemic conditions hamper keratinocyte locomotion via sequential inhibition of distinct pathways: New insights on poor wound closure in patients with diabetes, Br. J. Dermatol. 160 (6) (2009) 1206-1214.

[11] H.A. Thomason, N.H. Cooper, D.M. Ansell, M. Chui, A.J. Merrit, M.J. Hardman, D.R. Garrod, Direct evidence that PKCα positively regulates wound re-epithelialization: Correlation with changes in desmosomal adhesiveness, J. Pathol. 227 (3) (2012) 346-356.

[12] N.B. Menke, K.R. Ward, T.M. Witten, D.G. Bonchev, R.F. Diegelmann, Impaired wound healing, Clin. Dermatol. 25 (1) (2007) 19-25.

[13] C.K. Sen, G.M. Gordillo, S. Roy, R. Kirsner, L. Lambert, T.K. Hunt, F. Gottrup, G.C. Gurtner, M.T. Longaker, Human skin wounds: A major and snowballing threat to public health and the economy, Wound Rep. Regen. 17 (6) (2009) 763-771.

[14] M.B. Dreifke, A.A. Jayasuriya, A.C. Jayasuriya, Current wound healing procedures and potential care, Mater. Sci. Eng. C Mater. Biol. Appl. 48 (2015) 651-662.

[15] R.G. Frykberg, J. Banks, Challenges in the treatment of chronic wounds, Adv. Wound Care 4 (9) (2015) 560-582.

[16] P. Blume, M. Bowlby, B.M. Schmidt, R. Donegan, Safety and efficacy of Becaplermin gel in the treatment of diabetic foot ulcers, Chronic Wound Care Manag. Res. 2014 (1) (2014) 11-14.

[17] A.J. Whittam, Z.N. Maan, D. Duscher, V.W. Wong, J.A. Barrera, M. Januszyk, G.C. Gurtner, Challenges and opportunities in drug delivery for wound healing, Adv. Wound Care 5 (2) (2016) 79-88.

[18] J. Hardwicke, R. Moseley, P. Stephens, K. Harding, R. Duncan, D.W. Thomas, Bioresponsive dextrin-rhEGF conjugates: *In vitro* evaluation in models relevant to its proposed use as a treatment for chronic wounds, Mol. Pharm. 7 (3) (2010) 699-707.

[19] T. Mosmann, Rapid colorimetric assay for cellular growth and survival: Application to proliferation and cytotoxocity assays, J. Immunol. Methods 65 (1-2) (1983) 55-63.

[20] P.J. Smith, M. Wiltshire, R.J. Errington, DRAQ5 labeling of nuclear DNA in live and fixed cells, Curr. Protoc. Cytom. 28 (2004) 7.25.1-7.25.11.

Dataset [21] R. Moseley, Novel epoxy-tiglianes stimulate skin keratinocyte wound healing responses and re-epithelialization via protein kinase C activation (Supplementary Data), Mendeley Data, V1, 2019, *https://data.mendeley.com/datasets/gd8nxrt8z9/draft?a=4baf097e-063a-43df-a443-f27bb8164ec6*.

[22] H.H. Bragulla, D.G. Homberger, Structure and functions of keratin proteins in simple, stratified, keratinized and cornified epithelia, J. Anat. 214 (4) (2009) 516-559.

[23] F. Cajone, G.V. Sherbet, Stathmin is involved in S100A4-mediated regulation of cell cycle progression, Clin. Exp. Metastasis 17 (10) (1999) 865-871.

[24] J.R. Zibert, L. Skov, J.P. Thyssen, G.K. Jacobsen, M. Grigorian, Significance of the S100A4 protein in psoriasis, J. Invest. Dermatol. 130 (1) (2010) 150-160.

[25] I.M. Freedberg, M. Tomic-Canic, M. Komine, M. Blumenberg, Keratins and the keratinocyte activation cycle, J. Invest. Dermatol. 116 (5) (2001) 633-640.

[26] M.L. Usui, R.A. Underwood, J.N. Mansbridge, L.A. Muffley, W.G. Carter, J.E. Olerud, Morphological evidence for the role of suprabasal keratinocytes in wound reepithelialization, Wound Rep. Regen. 13 (5) (2005) 468-479.

[27] E. Candi, R. Schmidt, G. Melino, The cornified envelope: A model of cell death in the skin, Nat. Rev. Mol. Cell Biol. 6 (4) (2005) 328-340.

[28] K.K. Tan, G. Salgado, J.E. Connolly, J.K. Chan, E.B. Lane, Characterization of fetal keratinocytes, showing enhanced stem cell-like properties: A potential source of cells for skin reconstruction, Stem Cell Rep. 3 (2) (2014) 324-338.

[29] A. Turabelidze, S. Guo, A.Y. Chung, L. Chen, Y. Dai, P.T. Marucha, L.A. DiPietro, Intrinsic differences between oral and skin keratinocytes, PLoS One 9 (9) (2014) e101480.

[30] A. Waseem, B. Dogan, N. Tidman, Y. Alam, P. Purkis, S. Jackson, A. Lalli, M. Machesney, I.M. Leigh, Keratin 15 expression in stratified epithelia: Downregulation in activated keratinocytes, J. Invest. Dermatol. 112 (3) (1999) 362-369.

[31] M.M. van Rossum, J.M. Mommers, P.C. van de Kerkhof, P.E. van Erp, Coexpression of keratins 13 and 16 in human keratinocytes indicates association between hyperproliferation-associated and retinoid-induced differentiation, Arch. Dermatol. Res. 292 (1) (2000) 16-20.

[32] A. Bose, M.T. Teh, I.C. Mackenzie, A. Waseem, Keratin k15 as a biomarker of epidermal stem cells, Int. J. Mol. Sci. 14 (10) (2013) 19385-19398.

[33] F. Loschke, M. Homberg, T.M. Magin, Keratin isotypes control desmosome stability and dynamics through PKCα, J. Invest. Dermatol. 136 (1) (2016) 202-213.

[34] A. Trost, P. Desch, V. Wally, M. Haim, R.H. Maier, H.A. Reitsamer, H. Hintner, J.W. Bauer, K. Onder, Aberrant heterodimerization of keratin 16 with keratin 6A in HaCaT keratinocytes results in diminished cellular migration, Mech. Ageing Dev. 131 (5) (2010) 346-353.

[35] P. Wong, P.A. Coulombe, Loss of keratin 6 (K6) proteins reveals a function for intermediate filaments during wound repair, J. Cell Biol. 163 (2) (2003) 327-337.

[36] F. Wang, S. Chen, H.B. Liu, C.A. Parent, P.A. Coulombe, Keratin 6 regulates collective keratinocyte migration by altering cell-cell and cell-matrix adhesion, J. Cell Biol. 217 (12) (2018) 4314-4330.

[37] S. Mazzalupo, P. Wong, P. Martin, P.A. Coulombe, Role for keratins 6 and 17 during wound closure in embryonic mouse skin, Dev. Dyn. 226 (2) (2003) 356-365.

[38] D. Gong, J.E. Ferrell Jr, The roles of cyclin A2, B1, and B2 in early and late mitotic events, Mol. Biol. Cell 21 (18) (2010) 3149-3161.

[39] G. Nalepa, J. Barnholtz-Sloan, R. Enzor, D. Dey, Y. He, J.R. Gehlhausen, A.S. Lehmann, S.J. Park, Y. Yang, X. Yang, S. Chen, X. Guan, Y. Chen, J. Renbarger, F.C. Yang, L.F. Parada, W. Clapp, The tumor suppressor CDKN3 controls mitosis, J. Cell Biol. 201 (7) (2013) 997-1012.

[40] O. Cazzalini, A.I. Scovassi, M. Savio, L.A. Stivala, E. Prosperi, Multiple roles of the cell cycle inhibitor p21^{CDKN1A} in the DNA damage response, Mutat. Res. 704 (1-3) (2010) 12-20.

[41] P. Salaun, Y. Rannou, C. Prigent, Cdk1, Plks, Auroras, and Neks: The mitotic bodyguards, Adv. Exp. Med. Biol. 617 (2008) 41-56, (2008).

[42] A. Kumar, V. Rajendran, R. Sethumadhavan, R. Purohit, CEP proteins: The knights of centrosome dynasty, Protoplasma 250 (5) (2013) 965-983.

[43] X. Zhang, L. Zhong, B.Z. Liu, Y.J. Gao, Y.M. Gao, X.X. Hu, Effect of GINS2 on proliferation and apoptosis in leukemic cell line, Int. J. Med. Sci. 10 (12) (2013) 1795-1804.

[44] C. Xie, C. Powell, M. Yao, J. Wu, Q. Dong, Ubiquitin-conjugating enzyme E2C: A potential cancer biomarker, Int. J. Biochem. Cell Biol. 47 (2014) 113-117.

[45] J.J. Vincente, L. Wordeman, Mitosis, microtubule dynamics and the evolution of kinesins, Exp. Cell Res. 334 (1) (2015) 61-69.

[46] H. Neves, H.F. Kwok, In sickness and in health: The many roles of the minichromosome maintenance proteins, Biochim. Biophys. Acta Rev. Cancer 1868 (1) (2017) 295-308.

[47] U. Gaur, B.B. Aggarwal, Regulation of proliferation, survival and apoptosis by members of the TNF superfamily, Biochem. Pharmacol. 66 (2003) 1403-1408.

[48] O. Julien, J.A. Wells, Caspases and their substrates, Cell Death Differ. 24 (8) (2017) 1380-1389.

[49] H. Martinsson, M. Yhr, C. Enerbäck, Expression patterns of S100A7 (psoriasin) and S100A9 (calgranulin-B) in keratinocyte differentiation, Exp. Dermatol. 14 (3) (2005) 161-168.

[50] A. Voss, G. Bode, C. Sopalla, M. Benedyk, G. Varga, M. Böhm, W. Nacken, C. Kerkoff, Expression of S100A8/A9 in HaCaT keratinocytes alters the rate of cell proliferation and differentiation, FEBS Lett. 585 (2) (2011) 440-446.

[51] Q. Zhu, H.B. Mangukiya, D.S. Mashausi, H. Guo, H. Negi, S.B. Merugu, Z. Wu, D. Li, Anterior gradient 2 is induced in cutaneous wound and promotes wound healing through its adhesion domain, FEBS J 284 (17) (2017) 2856-2869.

[52] Q. Miao, A.T. Ku, Y. Nishino, J.M. Howard, A.S. Rao, T.M. Shaver, G.E. Garcia, D.N. Le, K.L. Karlin, T.F. Westbrook, V. Poli, H. Nguyen, Tcf3 promotes cell migration and wound repair through regulation of lipocalin 2, Nat. Commun. 5 (2014) 4088.

[53] M. Higaki, Y. Higaki, M. Kawashima, Increased expression of CD208 (DC-LAMP) in epidermal keratinocytes of psoriatic lesions, J. Dermatol. 36 (3) (2009) 144-149.

[54] E. Ogawa, Y. Owada, S. Ikawa, Y. AdachI, T. Egawa, K. Nemoto, K. Suzuki, T. Hishinuma, H. Kawashima, H. Kondo, M. Muto, S. Aiba, R. Okuyama, Epidermal FABP (FABP5) regulates keratinocyte differentiation by 13(S)-HODE-mediated activation of the NF-κB signaling pathway, J. Invest. Dermatol. 131 (3) (2011) 604-612.

[55] M. Pal, M.J. Tan, R.L. Huang, Y.Y. Goh, X.L. Wang, M.B. Tang, N.S. Tan, Angiopoietin-like 4 regulates epidermal differentiation, PLoS One 6 (9) (2011) e25377.

[56] G. Bart, L. Hämäläinen, L. Rauhala, P. Salonen, M. Kokkonen, T.W. Dunlop, P. Pehkonen, T. Kumlin, M.I. Tammi, S. Pasonen-Seppänen, R.H. Tammi, rClca2 is associated

with epidermal differentiation and is strongly downregulated by ultraviolet radiation, Br. J. Dermatol. 171 (2) (2014) 376-387.

[57] T.M. Scharadin, R.L. Eckert, TIG3: An important regulator of keratinocyte proliferation and survival, J. Invest. Dermatol. 134 (3) (2014) 1811-1816.

[58] B.K. Pilcher, J.A. Dumin, B.D. Sudbeck, S.M. Krane, H.G. Wilgus, W.C. Parks, The activity of collagenase-1 is required for keratinocyte migration on a type I collagen matrix, J. Cell Biol. 137 (6) (1997) 1445-1457.

[59] M. Krampert, W. Bloch, T. Sasaki, P. Bugnon, T. Rülicke, E. Wolf, M. Aumailley, W.C. Parks, S. Werner, Activities of the matrix metalloproteinase stromelysin-2 (MMP-10) in matrix degradation and keratinocyte organization in wounded skin, Mol. Biol. Cell 15 (12) (2004) 5242-5254.

[60] P. Chen, L.E. Abacherli, S.T. Nadler, Y. Wang, Q. Li, W.C. Parks, MMP7 shedding of syndecan-1 facilitates re-epithelialization by affecting $\alpha_2\beta_1$ integrin activation. PLoS One 4 (8) (2009) e6565.

[61] A. Pol, R. Pfundt, P. Zeeuwen, H. Molhuizen, J. Schalkwijk, Transcriptional regulation of the elafin gene in human keratinocytes, J. Invest. Dermatol. 120 (2) (2003) 301-307.

[62] S. Jang, T.H. Yang, E.J. An, H.K. Yoon, K.C. Sohn, A.Y. Cho, E.K. Ryu, Y.S. Park, T.Y. Yoon, J.H. Lee, C.D. Kim, Role of plasminogen activator inhibitor-2 (PAI-2) in keratinocyte differentiation, J. Dermatol. Sci. 59 (1) (2010), 25-30.

[63] C. Katagiri, T. Iida, J. Nakanishi, M. Ozawa, S. Aiba, T. Hibino, Up-regulation of serpin SCCA1 is associated with epidermal barrier disruption, J. Dermatol. Sci. 57 (2) (2010) 95-101.

[64] D.C. Hoffmann, C. Textoris, F. Oehme, T. Klaassen, A. Goppelt, A. Römer, B. Fugmann, J.M. Davidson, S. Werner, T. Krieg, S.A. Eming, Pivotal role for α_1-antichymotrypsin in skin repair, J. Biol. Chem. 286 (33) (2011) 28889-28901.

[65] U. Sivaprasad, K.G. Kinker, M.B. Ericksen, M. Lindsey, A.M. Gibson, S.A. Bass, N.S. Hershey, J. Deng, M. Medvedovic, G.K. Khurana Hershey, SERPINB3/B4 contributes to early inflammation and barrier dysfunction in an experimental murine model of atopic dermatitis, J. Invest. Dermatol. 135 (1) (2015) 160-169.

[66] K.A. Rubina, V.Y. Sysoeva, E.I. Zagorujko, Z.I. Tsokolaeva, M.I. Kurdina, Y.V. Parfyonova, V.A. Tkachuk, Increased expression of uPA, uPAR, and PAI-1 in psoriatic skin and in basal cell carcinomas, Arch. Dermatol. Res. 309 (6) (2017) 433-442.

[67] D. Breitkreutz, L. Braiman-Wiksman, N. Daum, M.F. Denning, T. Tennenbaum, Protein kinase C family: On the crossroads of cell signaling in skin and tumor epithelium, J. Cancer Res. Clin. Oncol. 133 (2007) 793-808.

[68] M.A. Lum, C.J Barger, A.H. Hsu, O.V. Leontieva, A.R. Black, J.D. Black, Protein kinase Cα (PKCα) is resistant to long term desensitization/down-regulation by prolonged diacylglycerol stimulation, J. Biol. Chem. 291 (12) (2016) 6331-6346.

[69] S.M. Fischer, M.L. Lee, R.E. Maldve, R.J. Morris, D. Trono, D.L. Burow, A.P. Butler, A. Pavone, B. Warren, Association of protein kinase C activation with induction of ornithine decarboxylase in murine but not human keratinocyte cultures, Mol. Carcinog. 7 (4) (1993) 228-237.

[70] H. Papp, G. Czifra, E. Bodó, J. Lázár, I. Kovács, M. Aleksza, I. Juhász, P. Acs, S. Sipka, L. Kovács, P.M. Blumberg, T. Bíró, Opposite roles of protein kinase C isoforms in proliferation, differentiation, apoptosis and tumorigenicity of human HaCaT keratinocytes, Cell. Mol. Life Sci. 61 (9) (2004) 1095-1105.

[71] A. Jerome-Morais, H.R. Rahn, S.S. Tibudan, M.F. Denning, Role for protein kinase C-α in keratinocyte growth arrest, J. Invest. Dermatol. 129 (10) (2009) 2365-2375.

[72] R. Sumagin, A.Z. Robin, A, Nusrat, C.A. Parkos, Activation of PKCβII by PMA facilitates enhanced epithelial wound repair through increased cell spreading and migration, PLoS One 8 (2) (2013) e55775.

Figure Legends

Fig. 1. (A) Chemical structures of epoxy-tiglianes, EBC-46 (tiglianol tiglate) and EBC-46 analogue, EBC-211 (produced by a Payne re-arrangement of the epoxide group on the β ring of EBC-46, circled in red). Stimulatory effects of epoxy-tiglianes on human skin keratinocyte (HaCaT) proliferation and cell cycle progression. (B-C) MTT analysis of HaCaT proliferation and viability, following treatment with 1.51 nM-151 µM EBC-46 and EBC-211 over 168 h, versus untreated HaCaTs. (D-E) DRAQ5™ and flow cytometry analysis of cell cycle progression and corresponding histogram depictions of % cells in each cell cycle phase, following HaCaT treatment with 1.51 nM-15.1 µM EBC-46 and EBC-211 for 40 h, versus untreated HaCaTs. See Supplementary Data from other cell cycle time-points analyzed, [21]. Results are presented as mean ± SEM, n=3 independent experiments. Significance at *$p<0.05$, **$p<0.01$ and ***$p<0.001$, versus untreated controls.

Fig. 2. Epoxy-tigliane enhancement of human skin keratinocyte (HaCaT) migration and scratch wound repopulation. (A) Representative Time-Lapse Microscopy images of HaCaT scratch wound repopulation at 48 h, following treatment with 1.51 nM-15.1 µM EBC-46 versus untreated HaCaTs (see Supplementary Videos S1 and S2 online for untreated and 1.51 nM EBC-46 scratch wounds over 48 h; and Supplementary Videos for 15.1 nM-15.1 µM EBC-46 treated HaCaTs, [21]). (B) ImageJ® analysis of HaCaT scratch wound repopulation and closure rates at 24 h and 48 h, following treatment with 1.51 nM-15.1 µM EBC-46 versus untreated HaCaTs. (C) Representative Time-Lapse Microscopy images of HaCaT scratch wound repopulation at 48 h, following treatment with 1.51 nM-15.1 µM EBC-211 versus untreated HaCaTs (see Supplementary Videos S3 and S4 online for untreated and 1.51 nM EBC-211 scratch wounds over 48 h; and Supplementary Videos for 15.1 nM-15.1 µM EBC-211 treated HaCaTs, [21]). (D) ImageJ® analysis of HaCaT scratch wound repopulation and closure rates at 24 h and 48 h, following treatment with 1.51 nM-15.1 µM EBC-211 versus untreated

HaCaTs. Results are presented as mean ± SEM, n=3 independent experiments. Significance at *p<0.05, **p<0.01 and ***p<0.001, versus untreated controls. White dashed lines show original scratch wound distances at 0 h. Scale bar = 100 μm.

Fig. 3. Epoxy-tigliane enhancement of human skin keratinocyte (HaCaT) migration and scratch wound repopulation, independently of increased proliferation. (A-B) ImageJ® analysis of HaCaT scratch wound repopulation and closure rates at 24 h and 48 h, following treatment with EBC-46 or EBC-211 (1.51 nM-15.1 μM) versus untreated HaCaTs, ± MC (see Supplementary Videos for untreated and 1.51 nM-15.1 μM EBC-46 and EBC-211 treated HaCaTs, [21]). Results are presented as mean ± SEM, n=3 independent experiments. Significance at *p<0.05, **p<0.01 and ***p<0.001, versus untreated controls.

Fig. 4. Epoxy-tiglianes modulate human skin keratinocyte (HaCaT) keratin gene and protein expression profiles to stimulate enhanced proliferation and migration. (A) Transcriptomic analysis by Illumina BeadChip Microarrays and heatmap visualization of genes differentially xpressed ≥2-fold by HaCaTs, following treatment with 1.51 nM, 151 nM or 15.1 μM EBC-46 or EBC-211 for 24 h and 48 h, versus untreated HaCaTs (based on n=4 independent profiling experiments for EBC-46 and EBC-211). (B) Western blot images and ImageJ® densitometric analysis of KRT13 protein levels, following HaCaT treatment with 1.51 nM-15.1 μM EBC-211 for 48 h, versus untreated HaCaTs. (C) Western blot images and ImageJ® densitometric analysis of KRT15 protein levels, following HaCaT treatment with 1.51 nM-15.1 μM EBC-211 for 24 h, versus untreated HaCaTs. For all Western blots, images from one representative experiment of three are shown. Results are presented as mean ± SEM, n=3 independent experiments. Significance at *p<0.05 versus untreated controls.

Fig. 5. Epoxy-tiglianes modulate human skin keratinocyte (HaCaT) cell cycle/proliferation-associated protein expression profiles to stimulate enhanced proliferation and migration. (A) Western blot images and ImageJ® densitometric analysis of cyclin A2 protein levels, following

HaCaT treatment with 1.51 nM-15.1 µM EBC-46 for 48 h, versus untreated HaCaTs. (B) Western blot images and ImageJ® densitometric analysis of cyclin B1 protein levels, following HaCaT treatment with 1.51 nM-15.1 µM EBC-46 for 24 h, versus untreated HaCaTs. (C) Western blot images and ImageJ® densitometric analysis of cyclin B2 protein levels, following HaCaT treatment with 1.51 nM-15.1 µM EBC-46 for 24 h and 48 h, versus untreated HaCaTs. (D) Western blot images and ImageJ® densitometric analysis of cyclin B2 protein levels, following HaCaT treatment with 1.51 nM-15.1 µM EBC-211 for 48 h, versus untreated HaCaTs. (E) Western blot images and ImageJ® densitometric analysis of CDKN1A protein levels, following HaCaT treatment with 1.51 nM-15.1 µM EBC-46 or EBC-211 for 24 h, versus untreated HaCaTs. For all Western blots, images from one representative experiment of three are shown. Results are presented as mean ± SEM, n=3 independent experiments. Significance at *$p<0.05$, **$p<0.01$ and ***$p<0.001$, versus untreated controls.

Fig. 6. Epoxy-tiglianes regulate MMP and S100 protein expression profiles in human skin keratinocytes (HaCaTs) to stimulate enhanced proliferation and migration. (A-C) MMP-1, MMP-7 and MMP-10 activities (activity assays), following HaCaT treatment with 1.51 nM-15.1 µM EBC-46 or EBC-211 for 24 h and 48 h, versus untreated HaCaTs. (D) Western blot images and ImageJ® densitometric analysis of S100A4 protein levels, following HaCaT treatment with 1.51 nM-15.1 µM EBC-46 for 24 h, versus untreated HaCaTs. (E) Western blot images and ImageJ® densitometric analysis of S100A8 protein levels, following HaCaT treatment with 1.51 nM-15.1 µM EBC-46 or EBC-211 for 48 h, versus untreated HaCaTs. For all Western blots, images from one representative experiment of three are shown. Results are presented as mean ± SEM, n=3 independent experiments. Significance at *$p<0.05$, **$p<0.01$ and ***$p<0.001$, versus untreated controls.

Fig. 7. Epoxy-tiglianes inhibit the expression and protein levels of key cytokine and chemokine agonists of human skin keratinocyte (HaCaT) proliferation and migration. (A-B) ELISA

analysis of selected cytokine (IL-6, IL-8) levels, following HaCaT treatment with 1.51 nM-15.1 µM EBC-46 or EBC-211 for 24 h and 48 h, versus untreated HaCaTs. (C-D) ELISA analysis of selected chemokine (CCL5, CXCL10) levels, following HaCaT treatment with 1.51 nM-15.1 µM EBC-46 or EBC-211 for 24 h and 48 h, versus untreated HaCaTs. Results are presented as mean ± SEM, n=3 independent experiments. Significance at *p<0.05, **p<0.01 and ***p<0.001, versus untreated controls.

Fig. 8. PKC activation mediates enhanced human skin keratinocyte (HaCaT) proliferative and migratory responses by epoxy-tiglianes. (A-B) MTT analysis of proliferation, following HaCaT treatment with 1.51 nM, 151 nM or 15.1 µM EBC-46 or EBC-211, over 72 h versus untreated HaCaTs, ± pan-PKC inhibitor, BIM-1 (1 µM). (C-D) Representative Time-Lapse Microscopy images and ImageJ® analysis of HaCaT scratch wound repopulation at 24h and 48 h, following treatment with 1.51 nM, 151 nM or 15.1 µM EBC-46, versus untreated HaCaTs over 48 h, ± BIM-1 (see Supplementary Videos for untreated and EBC-46-treated HaCaTs, [21]). (E-F) Representative Time-Lapse Microscopy images and ImageJ® analysis of HaCaT scratch wound repopulation at 24h and 48 h, following treatment with 1.51 nM, 151 nM or 15.1 µM EBC-211, versus untreated HaCaTs over 48 h, ± BIM-1 (see Supplementary Videos for untreated and EBC-211-treated HaCaTs, [21]). Results are presented as mean ± SEM, n=3 independent experiments. Significance at *p<0.05 and ***p<0.001, versus corresponding BIM-1-free controls. White dashed lines show original scratch wound distances at 0 h. Scale bar = 100 µm.

Fig. 9. PKC activation modulates keratin, cell cycle and MMP gene expression profiles by epoxy-tiglianes to enhance human skin keratinocyte (HaCaT) proliferation and migration. (A) Western blot images and ImageJ® densitometric analysis of KRT17 protein levels, following HaCaT treatment with 1.51 nM, 151 nM or 15.1 µM EBC-46 or EBC-211 for 24 h, versus untreated HaCaTs, ± pan-PKC inhibitor, BIM-1 (1 µM). (B) Western blot images and ImageJ®

densitometric analysis of cyclin B1 protein levels, following HaCaT treatment with 1.51 nM, 151 nM or 15.1 µM EBC-211 for 48 h, versus untreated HaCaTs, ± pan-PKC inhibitor, BIM-1. (C) Western blot images and ImageJ® densitometric analysis of CDKN1A protein levels, following HaCaT treatment with 1.51 nM, 151 nM or 15.1 µM EBC-46 for 24 h and 48 h, versus untreated HaCaTs, ± pan-PKC inhibitor, BIM-1. (D) Western blot images and ImageJ® densitometric analysis of CDKN1A protein levels, following HaCaT treatment with 1.51 nM, 151 nM or 15.1 µM EBC-211 for 48 h, versus untreated HaCaTs, ± pan-PKC inhibitor, BIM-1. (E-G) MMP-1, MMP-7 and MMP-10 activities (activity assays), following HaCaT treatment with 1.51 nM, 151 nM or 15.1 µM EBC-46 or EBC-211 for 48 h, versus untreated HaCaTs, ± BIM-1. For all Western blots, images from one representative experiment of three are shown. Results are presented as mean ± SEM, n=3 independent experiments. Significance at *$p<0.05$, **$p<0.01$ and ***$p<0.001$, versus corresponding BIM-1-free controls.

Fig. 10. PKC phosphorylation and activation profiles induced by epoxy-tiglianes to enhance human skin keratinocyte (HaCaT) proliferation and migration. (A-B) Western blot images and ImageJ® densitometric analysis of pan-PKC phosphorylation, following HaCaT treatment with 1.51 nM, 151 nM or 15.1 µM EBC-46 or EBC-211 over 24 h, versus untreated HaCaTs. For all Western blots, images from one representative experiment of three are shown. Results are presented as mean ± SEM, n=3 independent experiments.

Fig. 1A

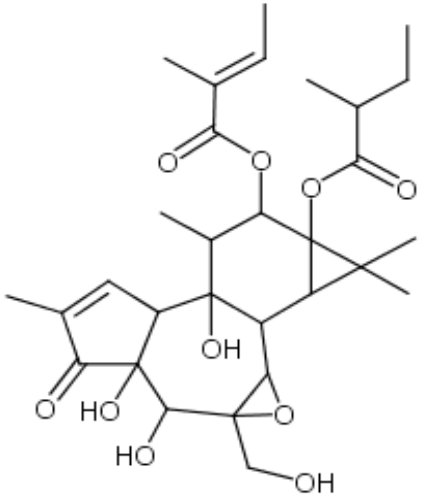

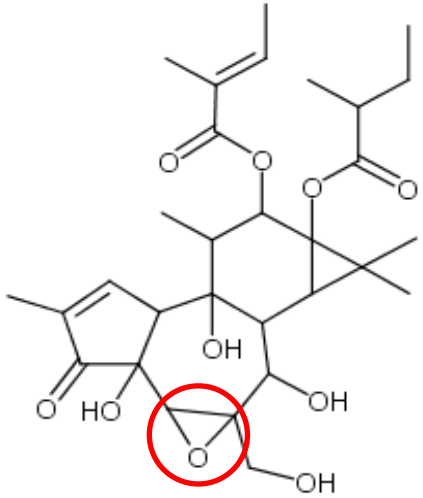

Fig. 1B

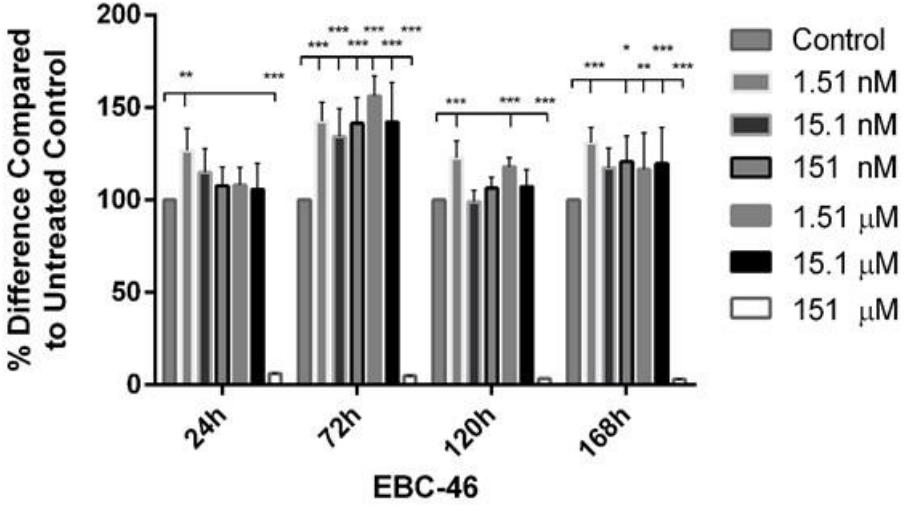

Fig. 1C

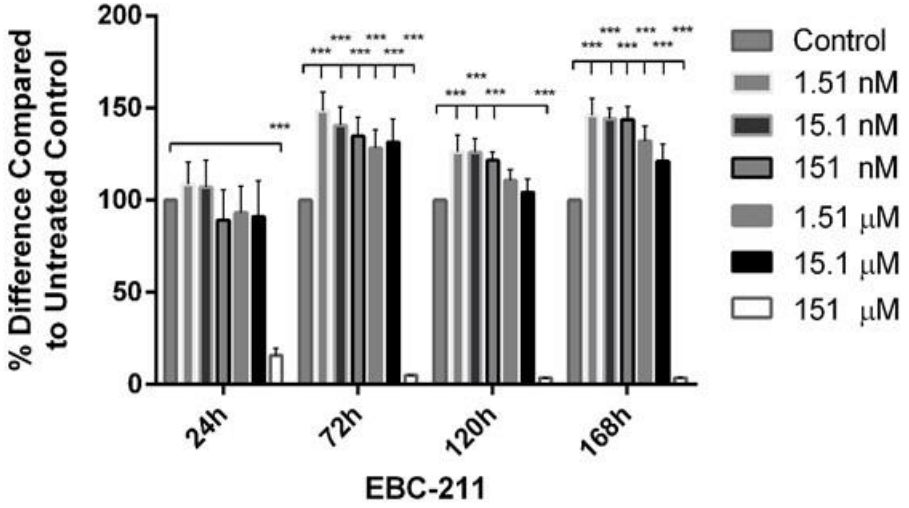

Fig. 1D

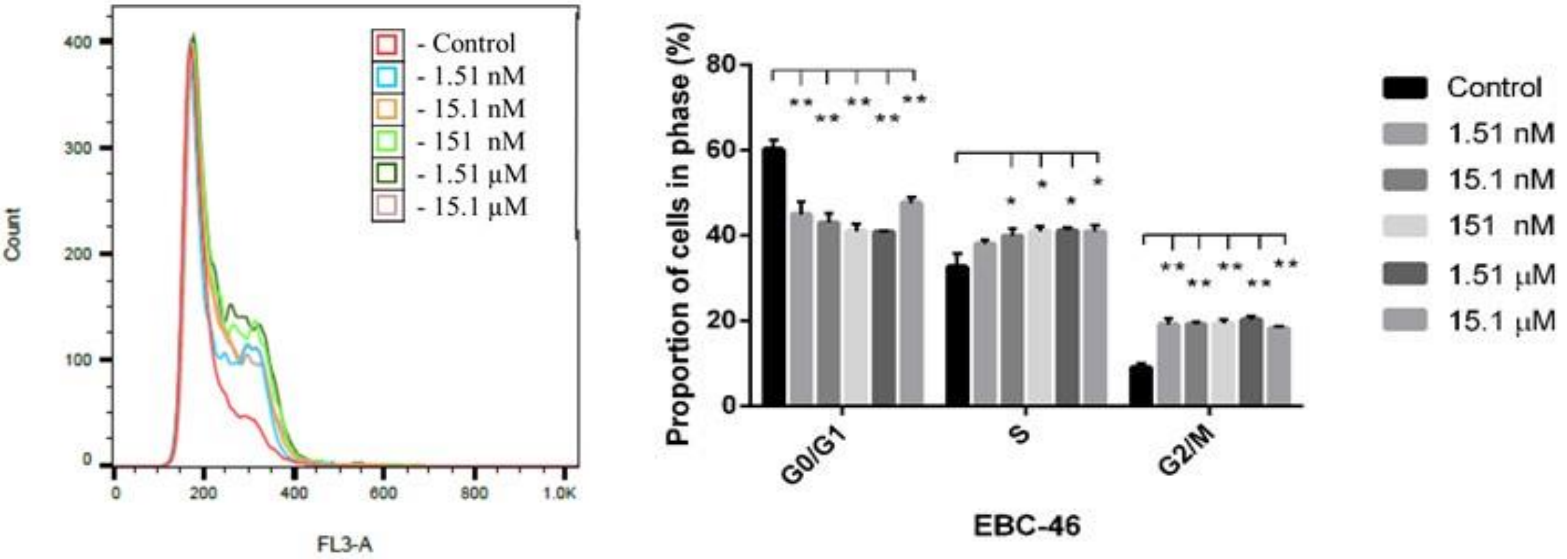
- Control
- 1.51 nM
- 15.1 nM
- 151 nM
- 1.51 µM
- 15.1 µM
Count
FL3-A
Proportion of cells in phase (%)
G0/G1
S
G2/M
EBC-46
Control
1.51 nM
15.1 nM
151 nM
1.51 µM
15.1 µM

Fig. 1E

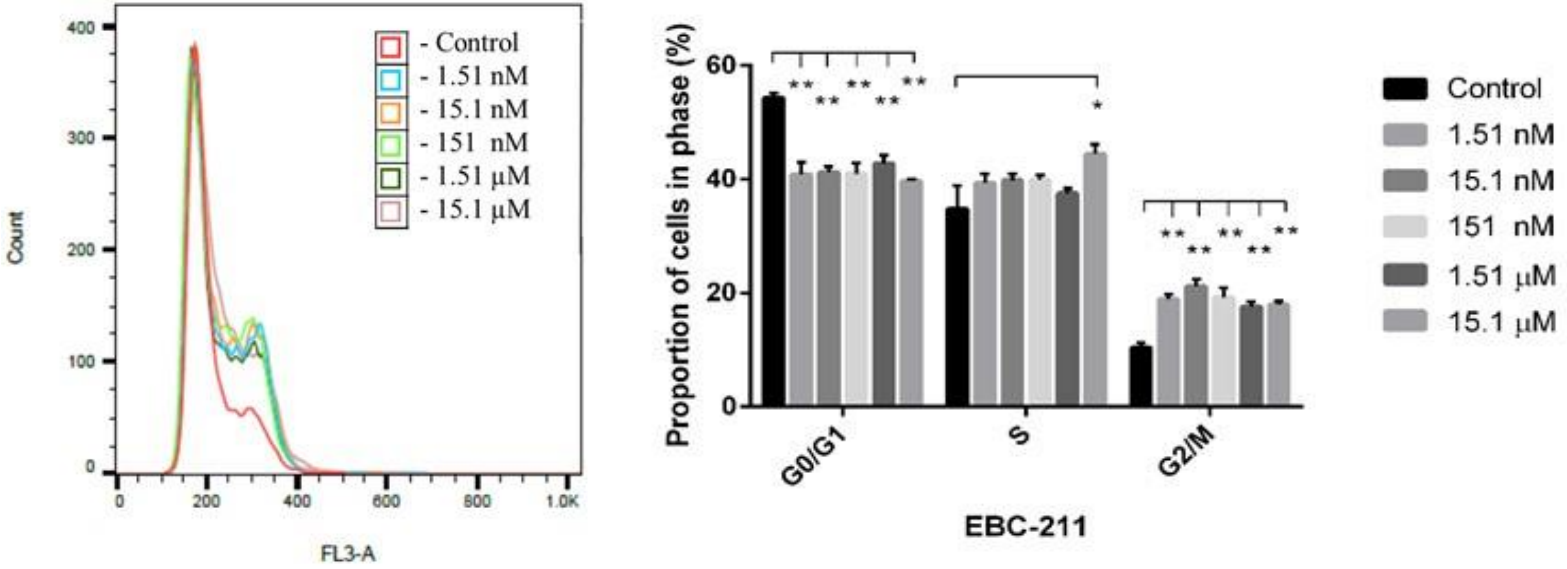
- Control
- 1.51 nM
- 15.1 nM
- 151 nM
- 1.51 µM
- 15.1 µM
Count
FL3-A
Proportion of cells in phase (%)
G0/G1
S
G2/M
EBC-211
Control
1.51 nM
15.1 nM
151 nM
1.51 µM
15.1 µM

Fig. 2A

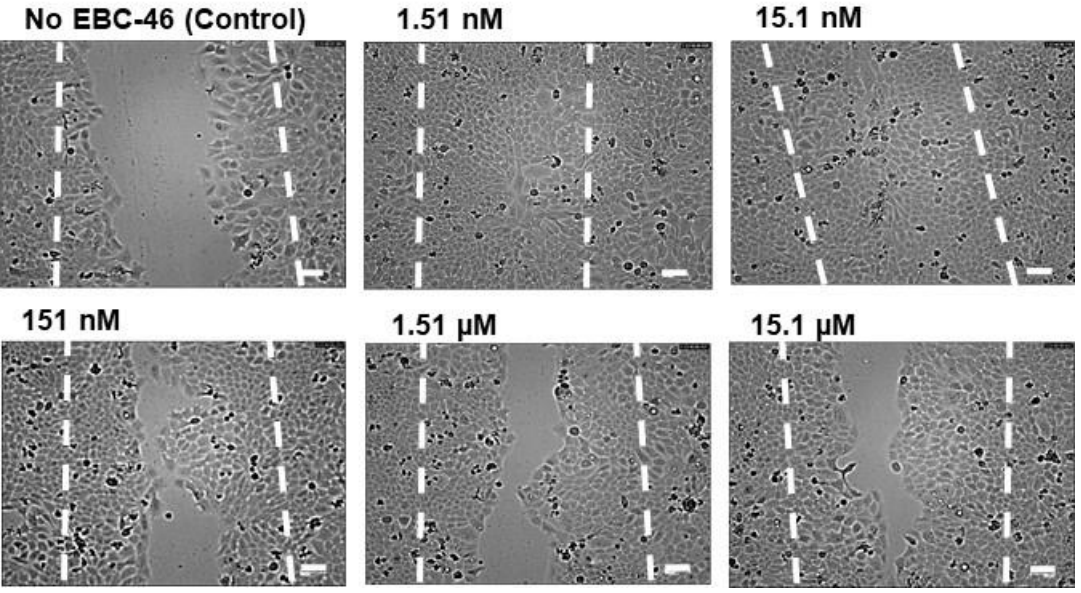

Fig. 2B

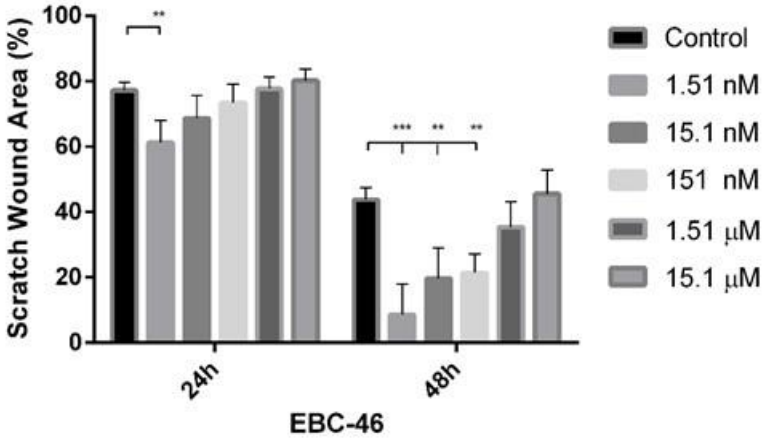

Fig. 2C

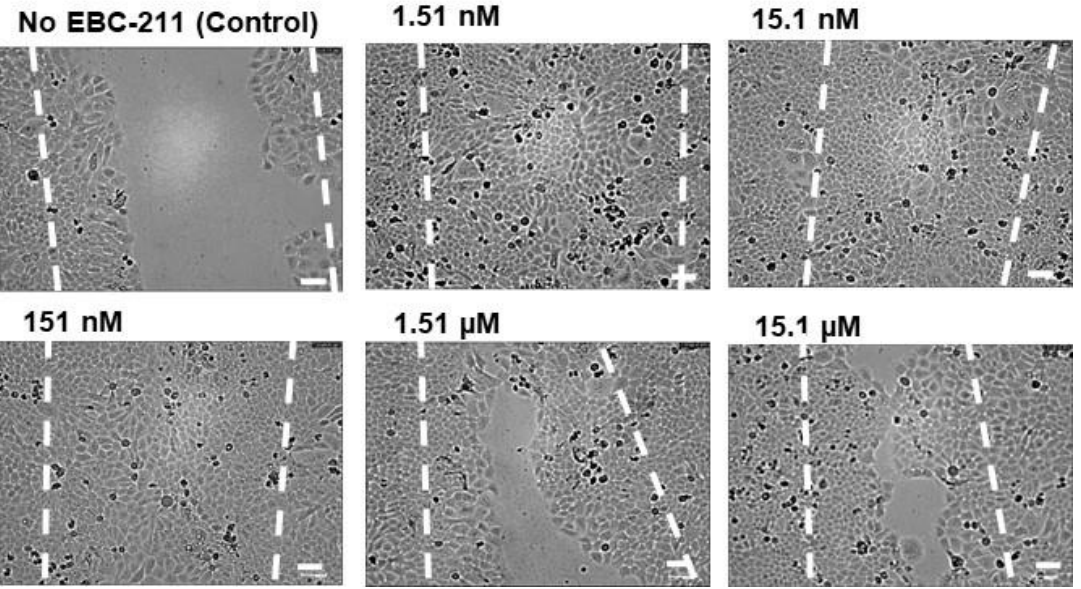

Fig. 2D

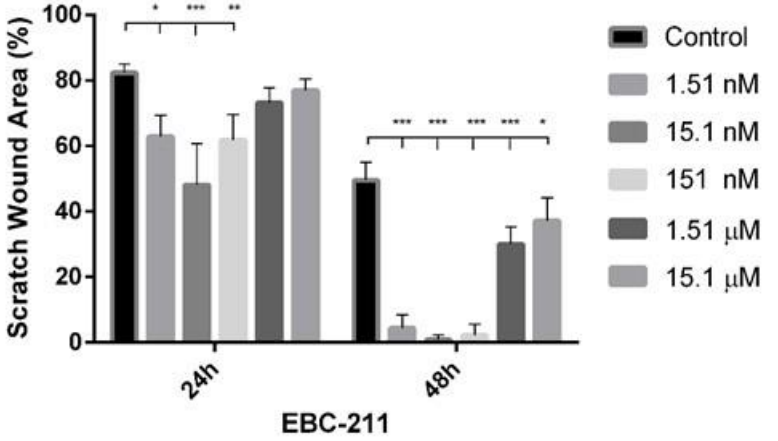

Fig. 3A

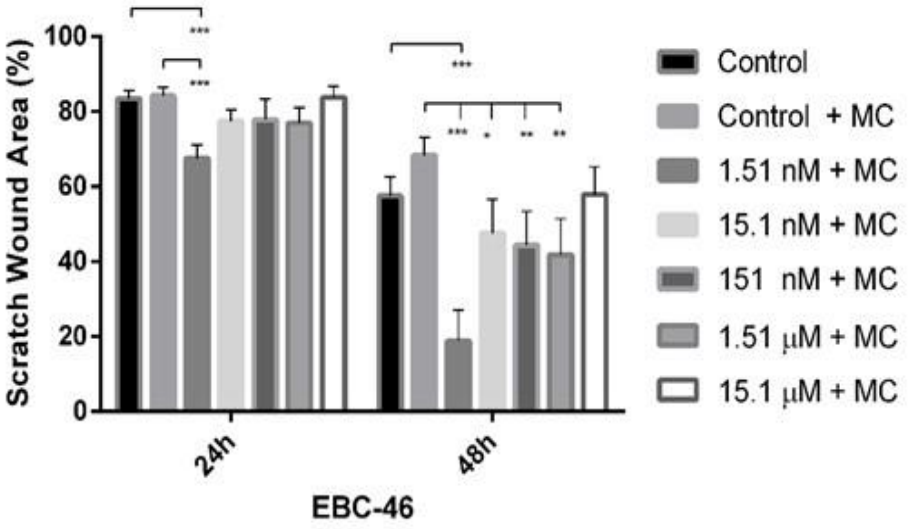
Scratch Wound Area (%)
100
80
60
40
20
0
24h
48h
EBC-46
Control
Control + MC
1.51 nM + MC
15.1 nM + MC
151 nM + MC
1.51 μM + MC
15.1 μM + MC

Fig. 3B

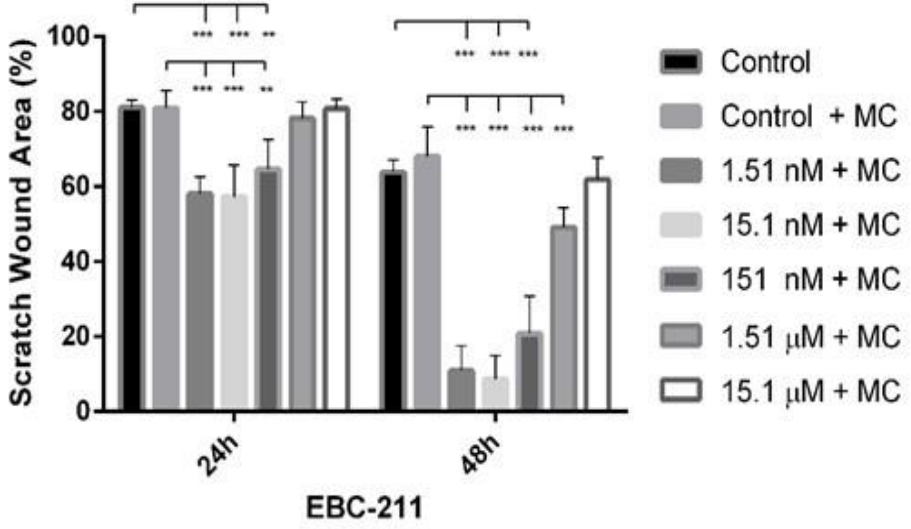
Scratch Wound Area (%)
100
80
60
40
20
0
24h
48h
EBC-211
Control
Control + MC
1.51 nM + MC
15.1 nM + MC
151 nM + MC
1.51 μM + MC
15.1 μM + MC

Fig. 4A

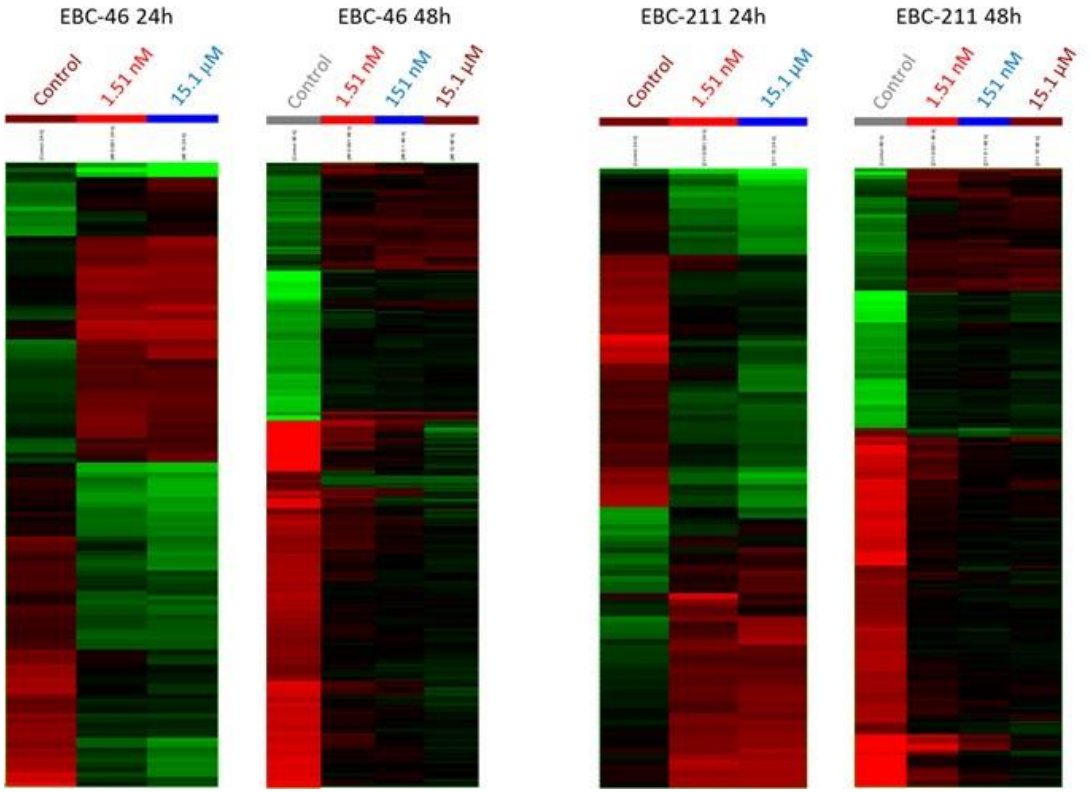

Fig. 4B

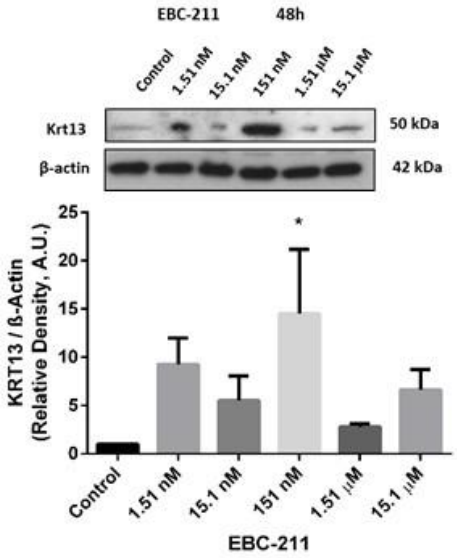

Fig. 4C

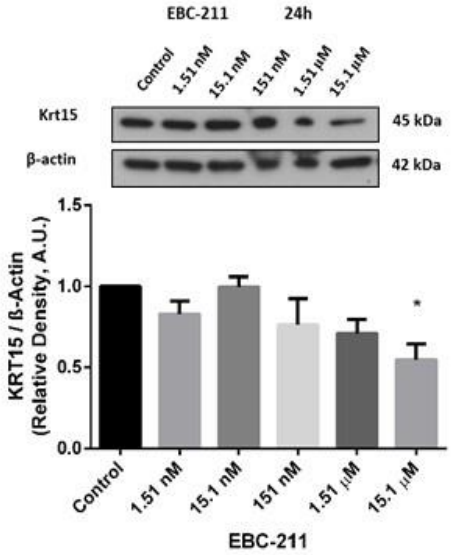

Fig. 5A

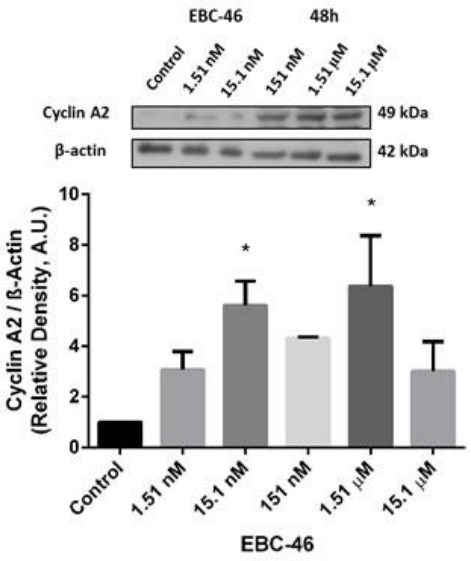

Fig. 5C

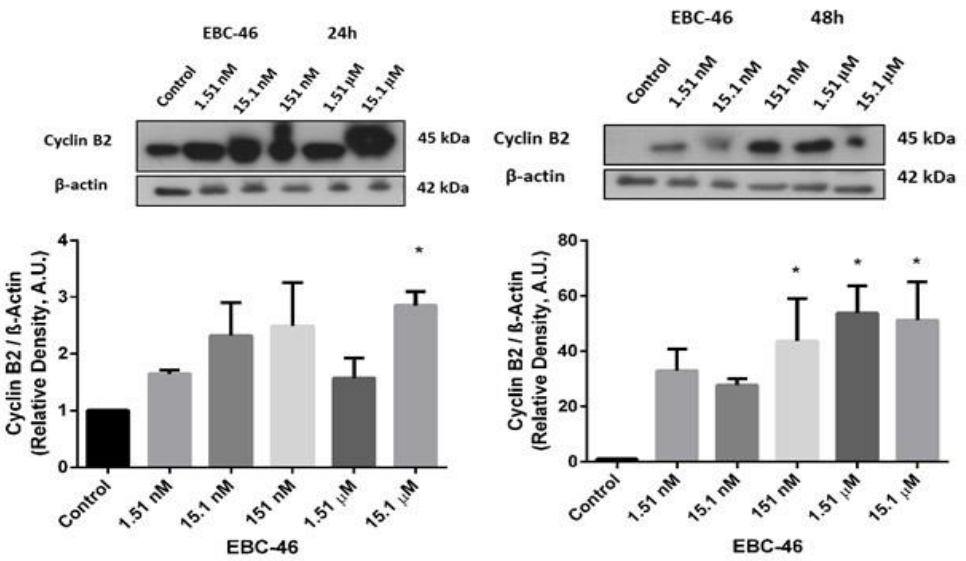

Fig. 5B

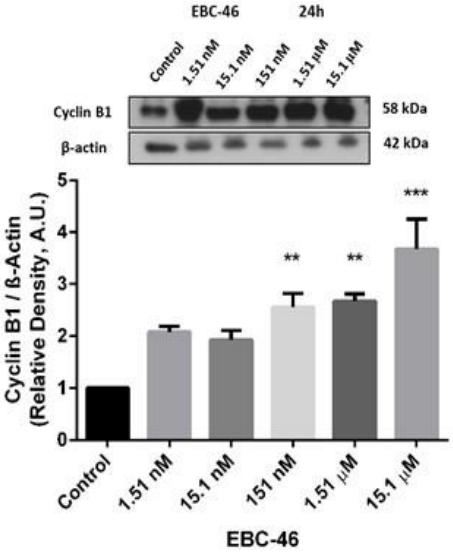

Fig. 5D

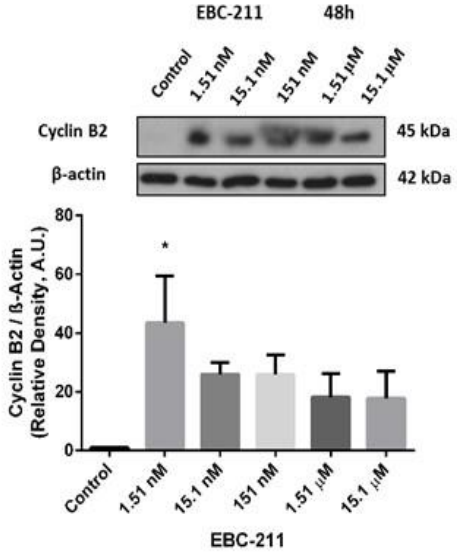

Fig. 5E

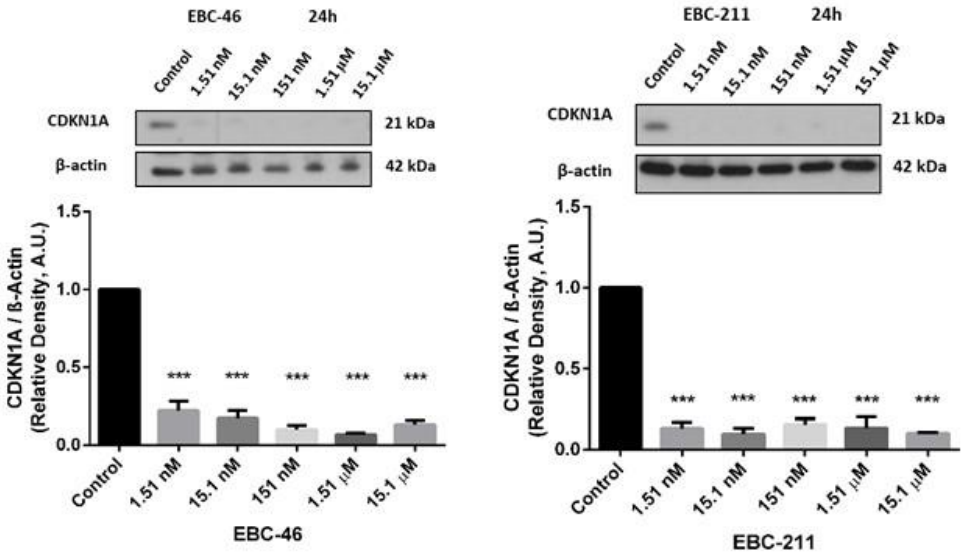
EBC-46
24h
Control
1.51 nM
15.1 nM
151 nM
1.51 µM
15.1 µM
CDKN1A
21 kDa
β-actin
42 kDa
CDKN1A / ß-Actin
(Relative Density, A.U.)
1.5
1.0
0.5
0.0
***
Control
1.51 nM
15.1 nM
151 nM
1.51 µM
15.1 µM
EBC-46
EBC-211
24h
Control
1.51 nM
15.1 nM
151 nM
1.51 µM
15.1 µM
CDKN1A
21 kDa
β-actin
42 kDa
CDKN1A / ß-Actin
(Relative Density, A.U.)
1.5
1.0
0.5
0.0
***
Control
1.51 nM
15.1 nM
151 nM
1.51 µM
15.1 µM
EBC-211

Fig. 6A

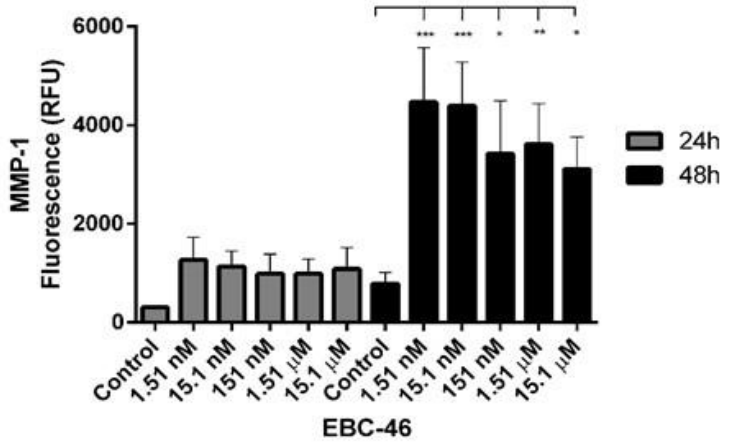

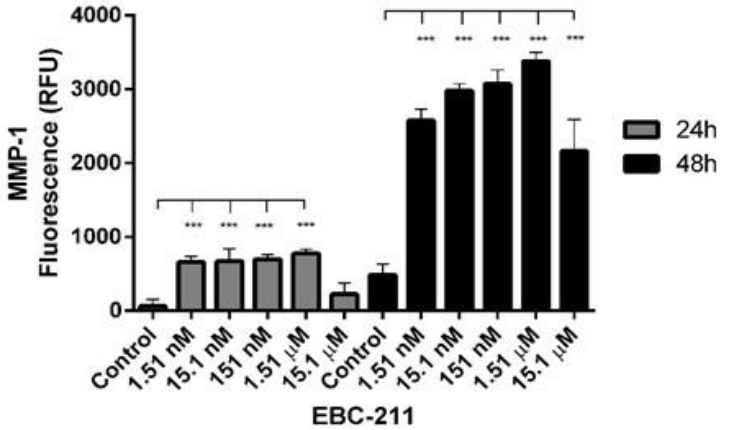

Fig. 6B

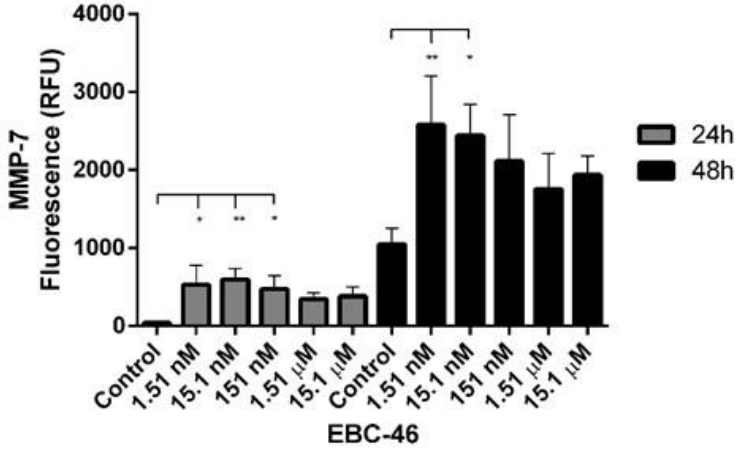

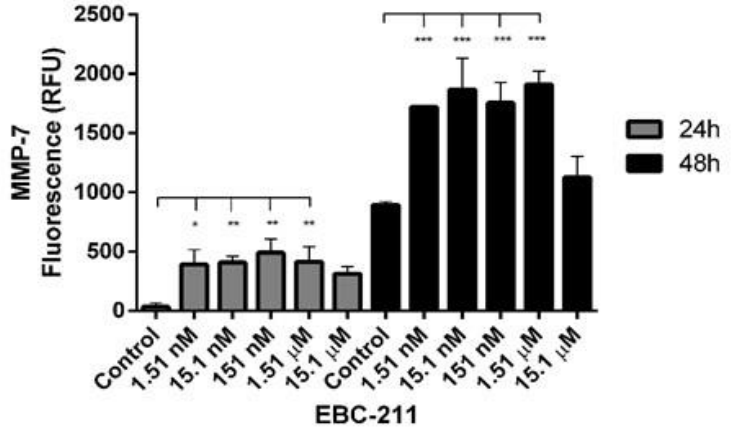

Fig. 6C

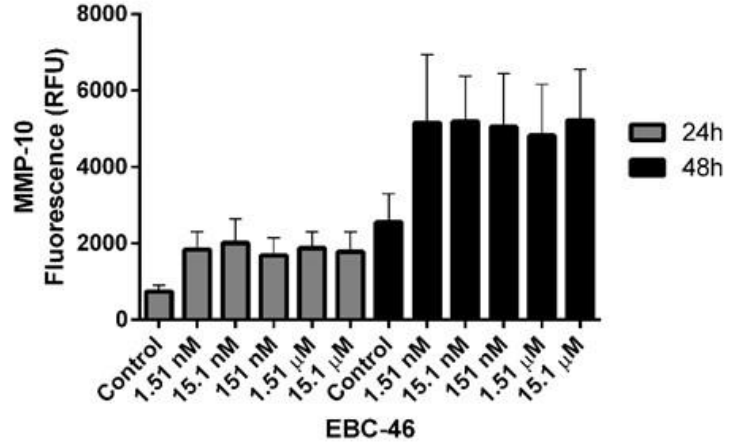

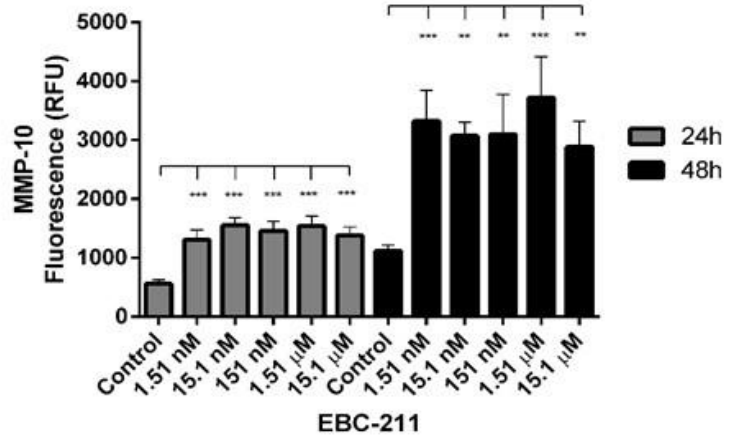

Fig. 6D

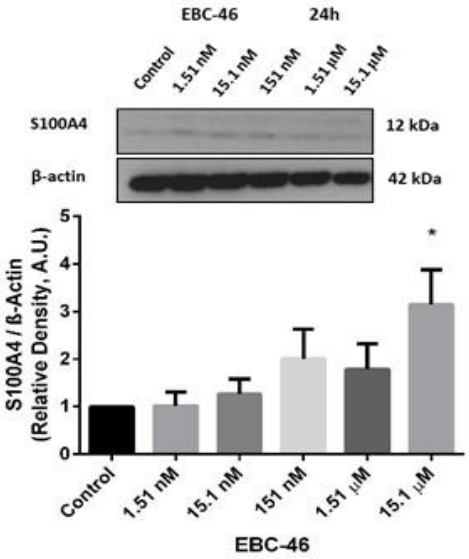
EBC-46
24h
Control
1.51 nM
15.1 nM
151 nM
1.51 µM
15.1 µM
S100A4
12 kDa
β-actin
42 kDa
S100A4 / ß-Actin (Relative Density, A.U.)
*
EBC-46

Fig. 6E

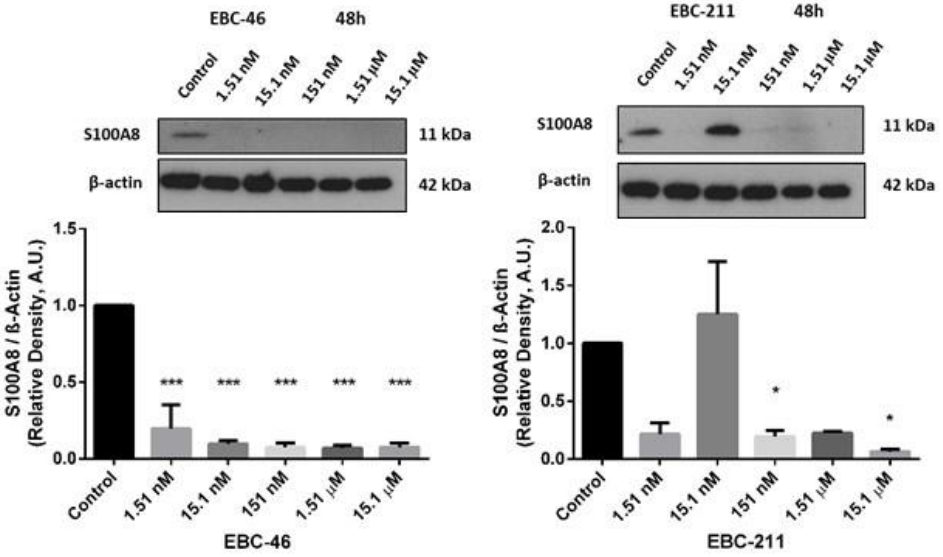
EBC-46
48h
Control
1.51 nM
15.1 nM
151 nM
1.51 µM
15.1 µM
S100A8
11 kDa
β-actin
42 kDa
S100A8 / ß-Actin (Relative Density, A.U.)
***
EBC-46
EBC-211
48h
S100A8
11 kDa
β-actin
42 kDa
S100A8 / ß-Actin (Relative Density, A.U.)
*
EBC-211

Fig. 7A

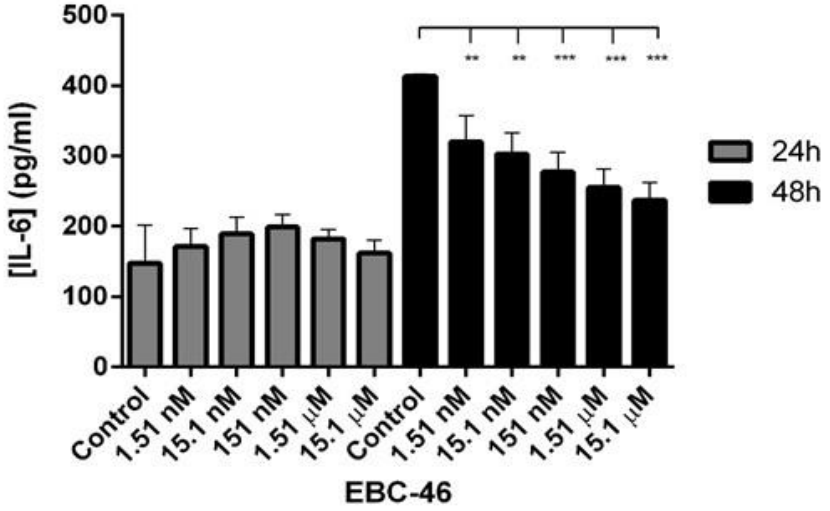
[IL-6] (pg/ml)
500
400
300
200
100
0
24h
48h
Control
1.51 nM
15.1 nM
151 nM
1.51 µM
15.1 µM
EBC-46

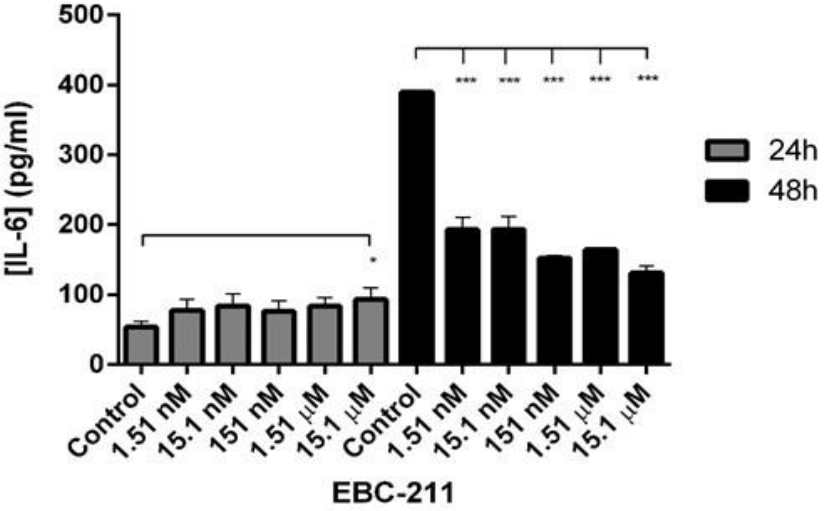
[IL-6] (pg/ml)
500
400
300
200
100
0
24h
48h
Control
1.51 nM
15.1 nM
151 nM
1.51 µM
15.1 µM
EBC-211

Fig. 7B

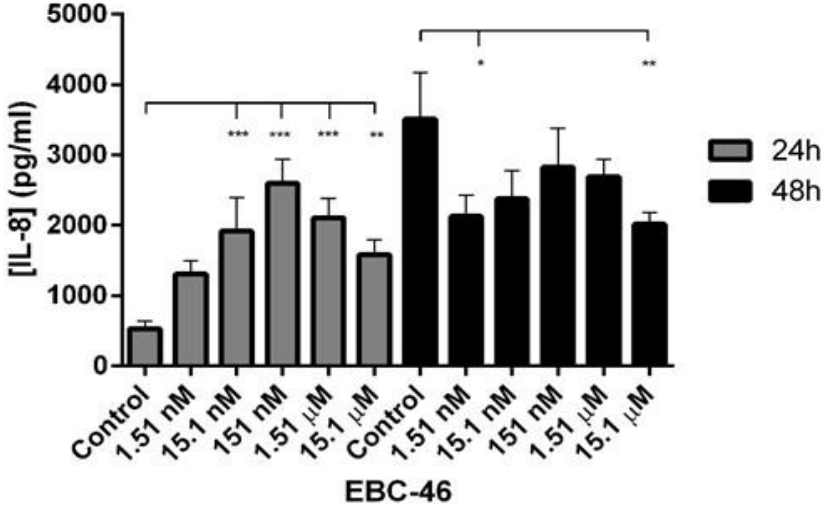
[IL-8] (pg/ml)
5000
4000
3000
2000
1000
0
24h
48h
Control
1.51 nM
15.1 nM
151 nM
1.51 µM
15.1 µM
EBC-46

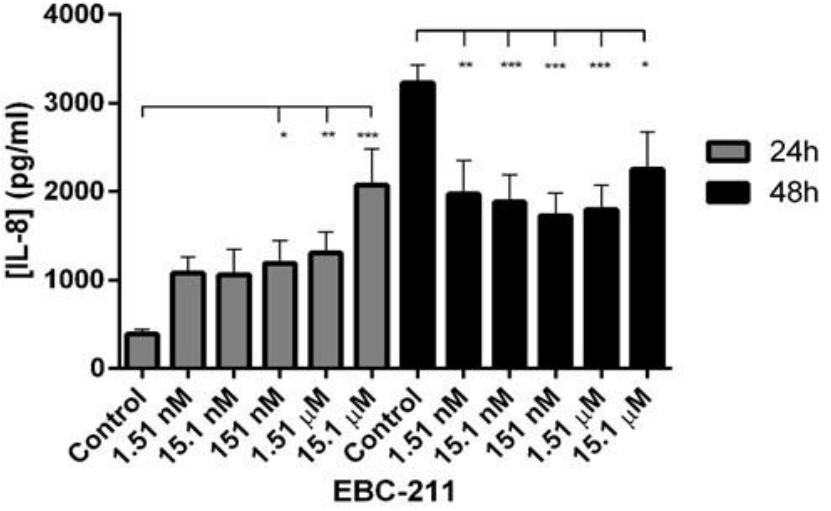
[IL-8] (pg/ml)
4000
3000
2000
1000
0
24h
48h
Control
1.51 nM
15.1 nM
151 nM
1.51 µM
15.1 µM
EBC-211

Fig. 7C

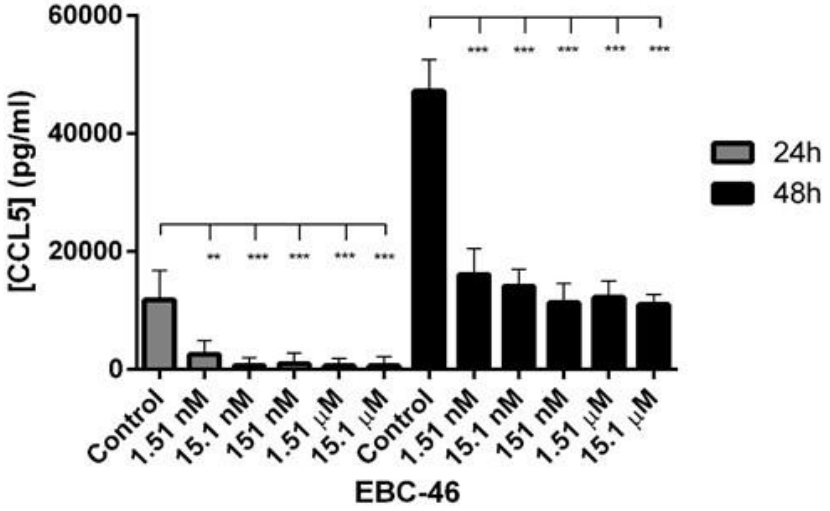
[CCL5] (pg/ml)
60000
40000
20000
0
24h
48h
Control
1.51 nM
15.1 nM
151 nM
1.51 µM
15.1 µM
EBC-46

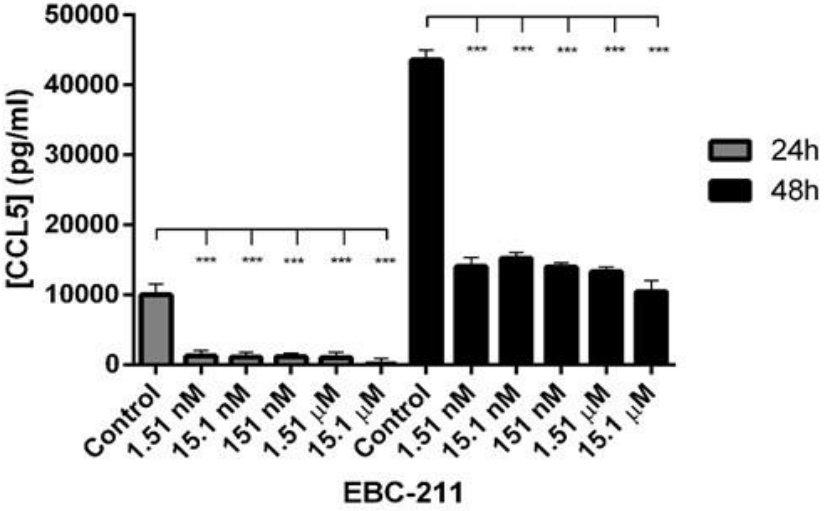
[CCL5] (pg/ml)
50000
40000
30000
20000
10000
0
24h
48h
Control
1.51 nM
15.1 nM
151 nM
1.51 µM
15.1 µM
EBC-211

Fig. 7D

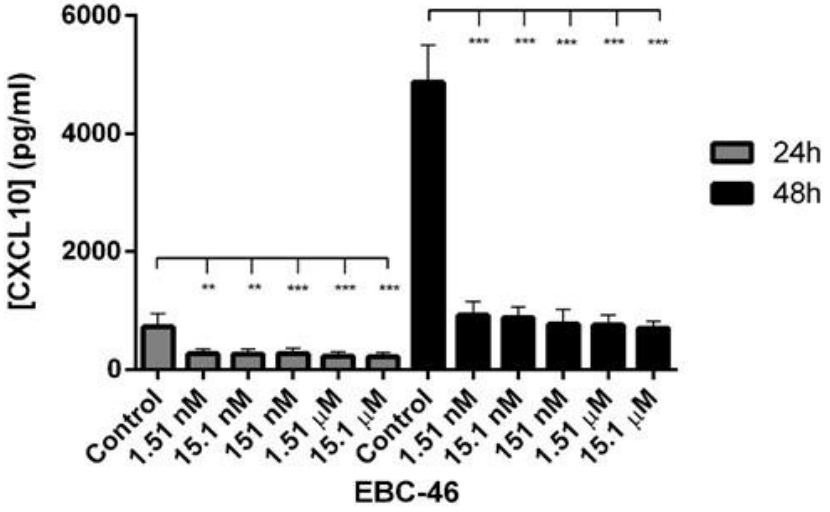
[CXCL10] (pg/ml)
6000
4000
2000
0
24h
48h
Control
1.51 nM
15.1 nM
151 nM
1.51 µM
15.1 µM
EBC-46

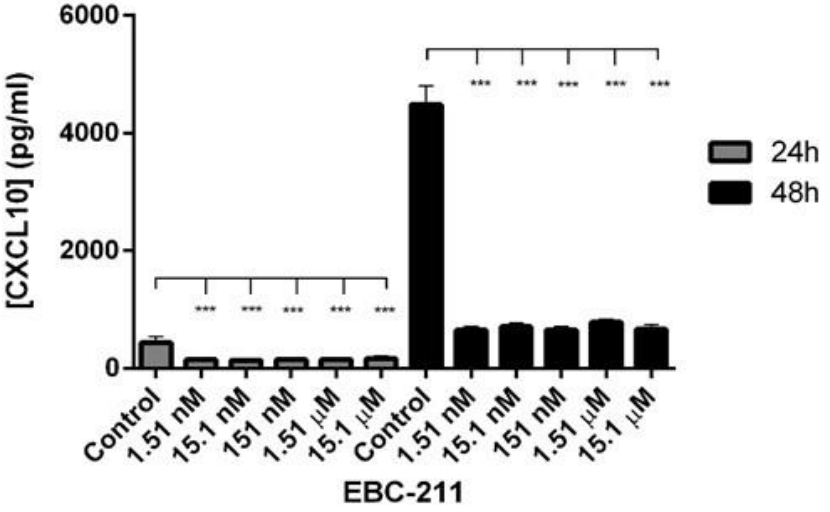
[CXCL10] (pg/ml)
6000
4000
2000
0
24h
48h
Control
1.51 nM
15.1 nM
151 nM
1.51 µM
15.1 µM
EBC-211

Fig. 8A

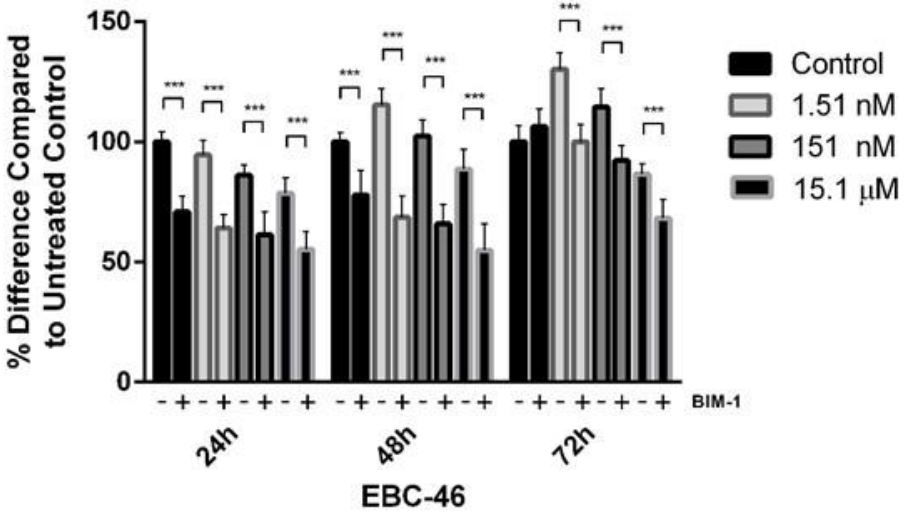

Fig. 8B

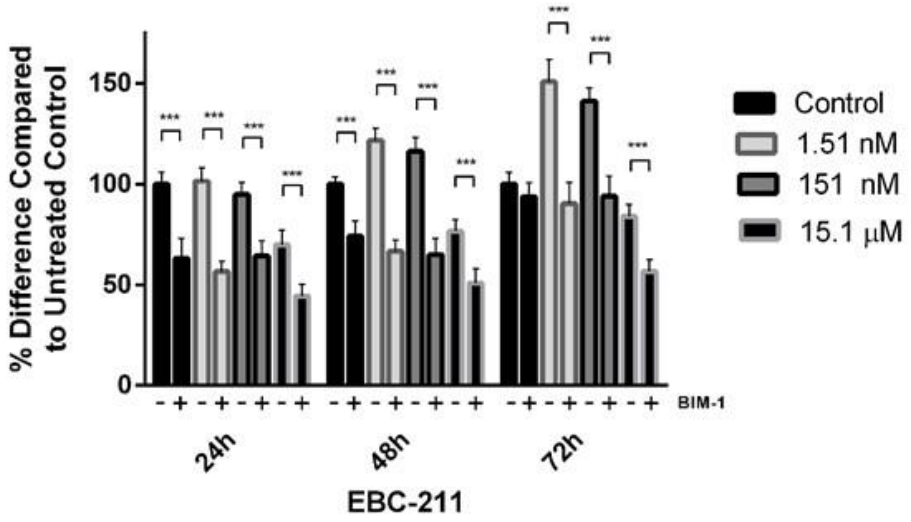

Fig. 8C

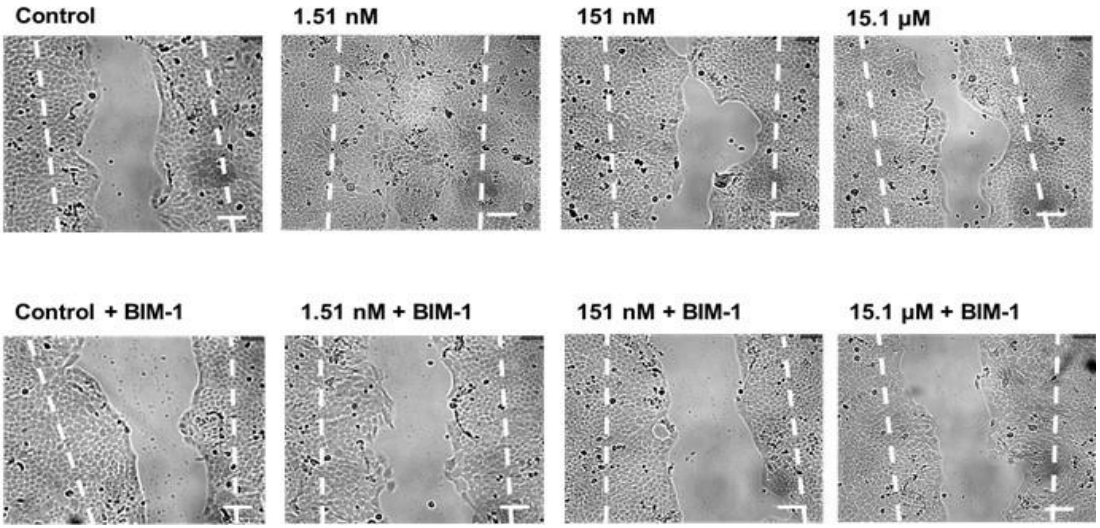

Fig. 8D

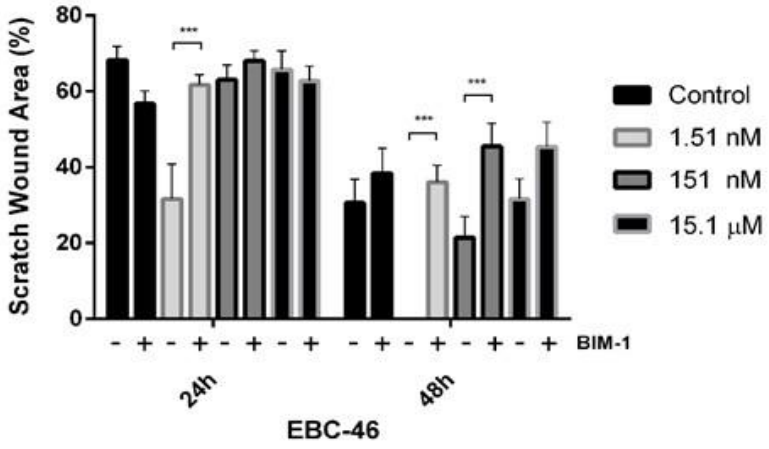

Fig. 8E

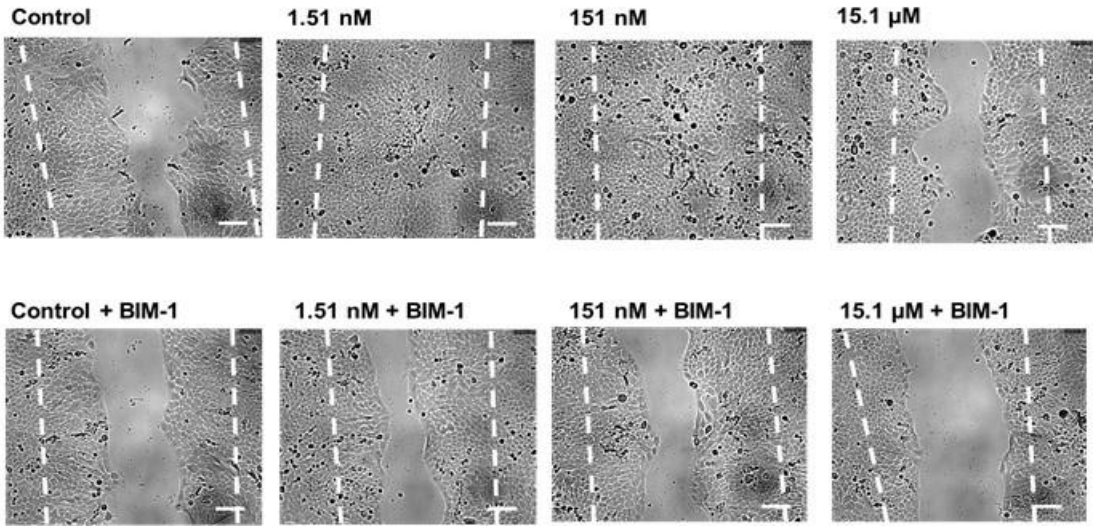
Control
1.51 nM
151 nM
15.1 µM
Control + BIM-1
1.51 nM + BIM-1
151 nM + BIM-1
15.1 µM + BIM-1

Fig. 8F

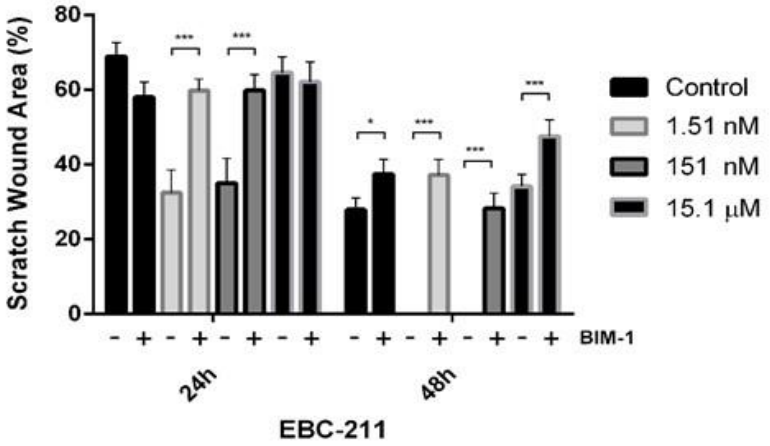
Scratch Wound Area (%)
80
60
40
20
0
***
***
*
***
***
***
- + - + - + - + - + - + - + - +
BIM-1
24h
48h
EBC-211
Control
1.51 nM
151 nM
15.1 µM

Fig. 9A

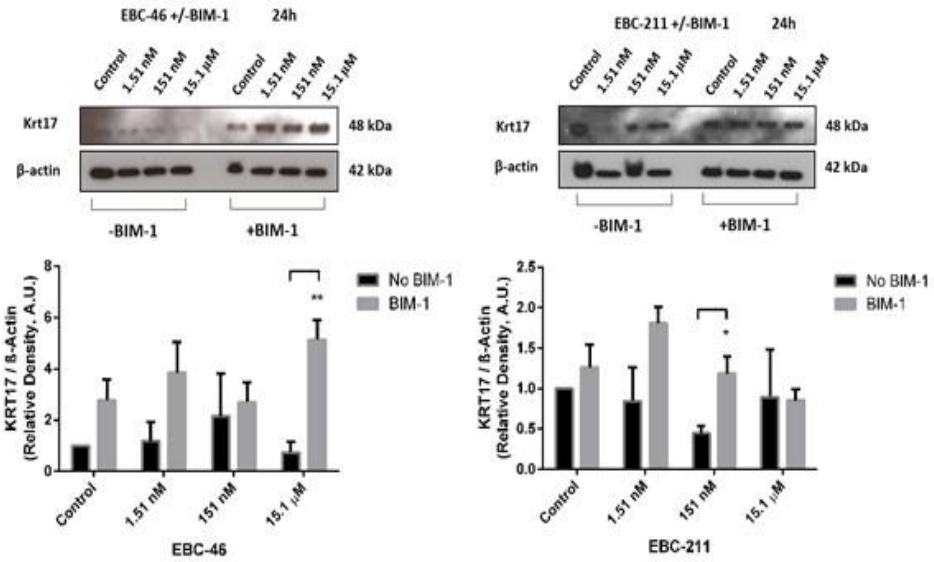

Fig. 9B

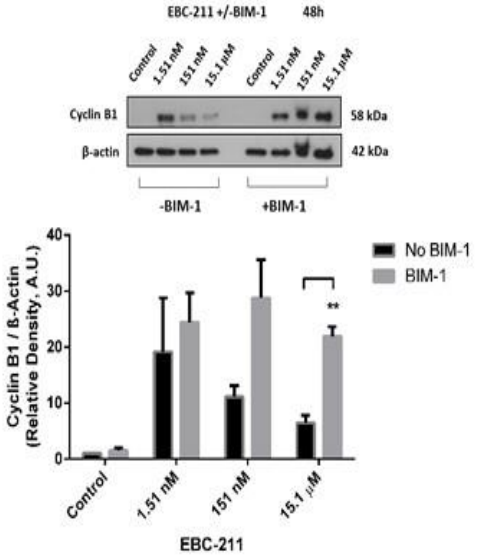

Fig. 9C

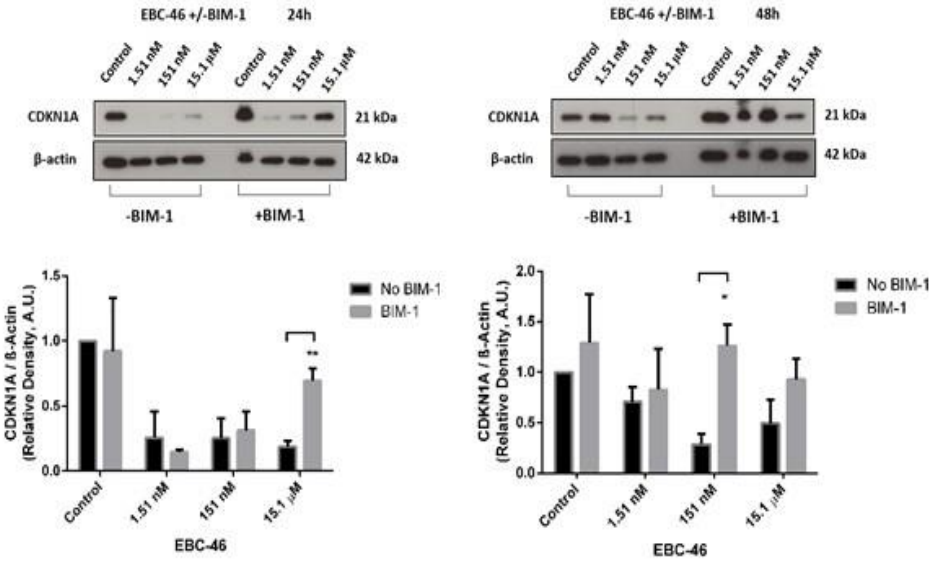

Fig. 9D

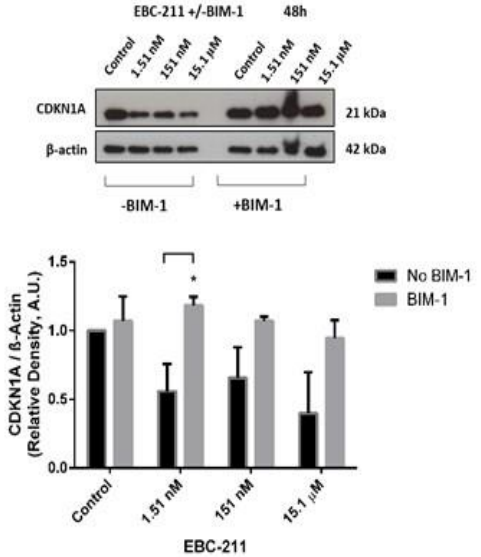

Fig. 9E

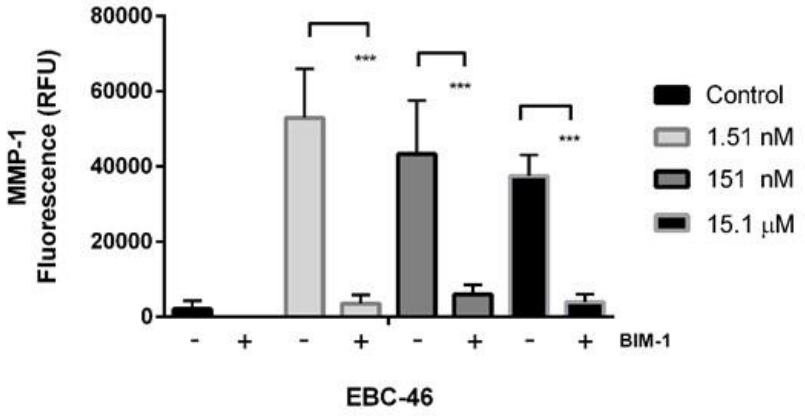

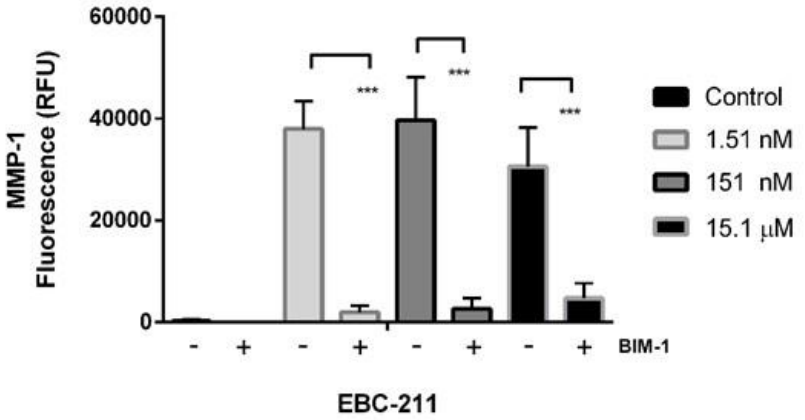

Fig. 9F

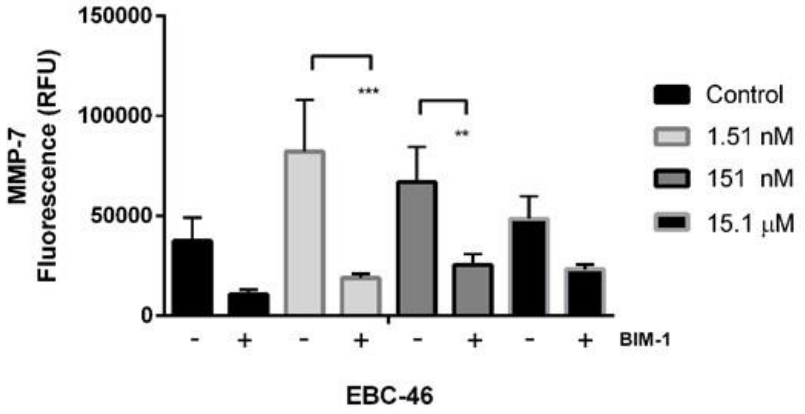

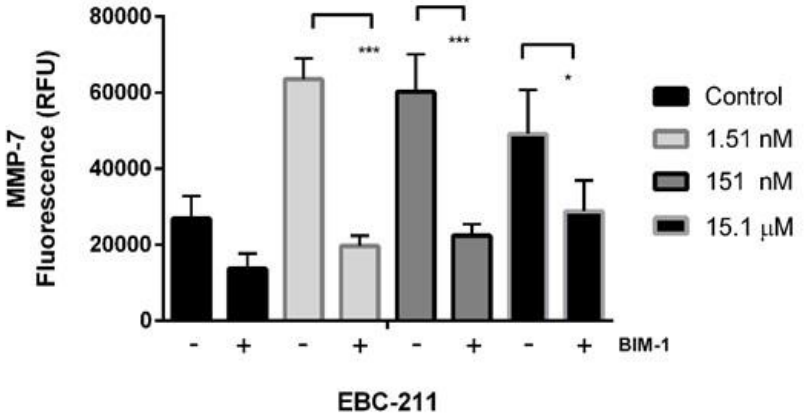

Fig. 9G

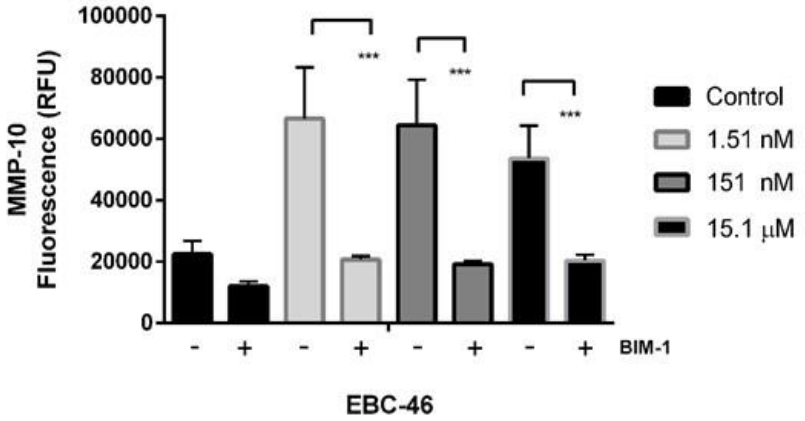

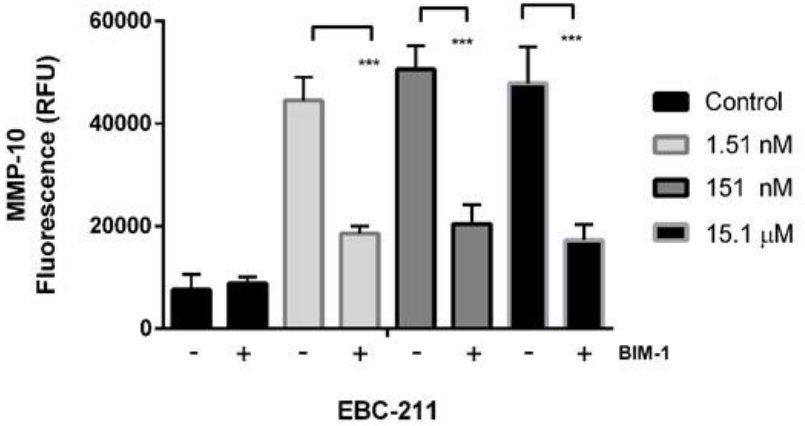

Fig. 10A

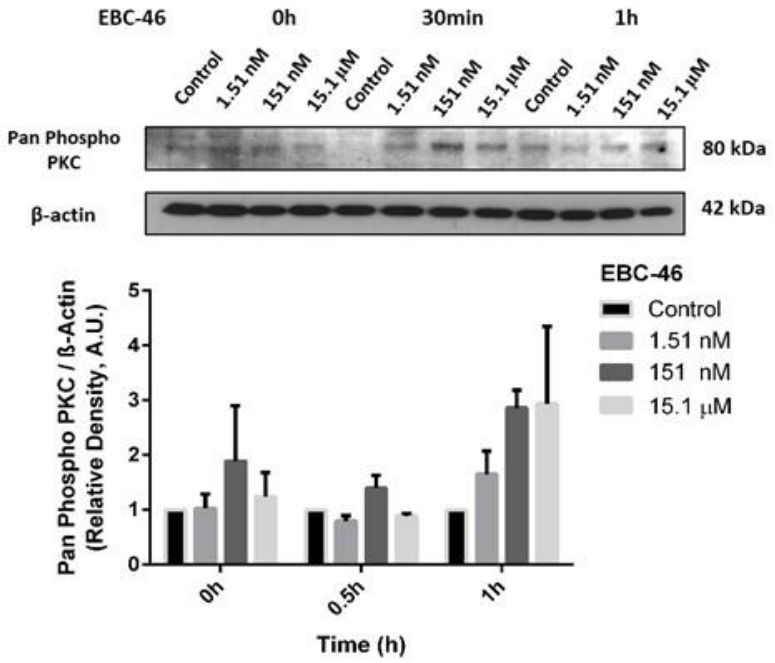

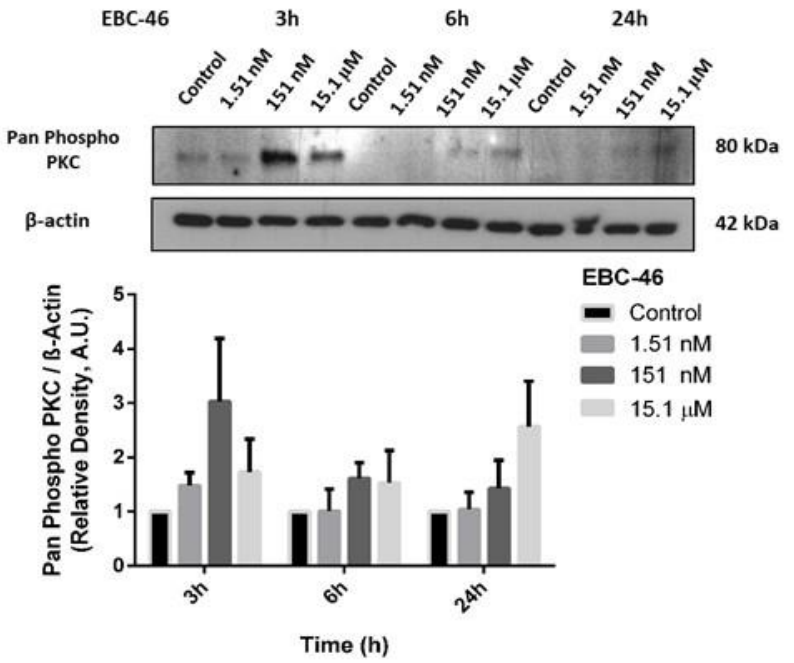

Fig. 10B